ABSTRACT

STEVENS, CAMERON LEE. Oligo(ethylene glycol) Grafted Polyester Polymer Brushes as Dynamic Surfaces. (Under the direction of Christopher Gorman).

A new route to oligo(ethylene glycol) appended α-hydroxy acids has been created. Conditions to generate cyclic monomers with these newly formed α-hydroxy acids were explored. Additionally, growth of a known *O*-carboxy anhydride moiety was tested for polymer brush growth.

Degradable polyester polymer brushes are a versatile platform for exploring protein resistance and understanding fundamental surface structure property relationships. Poly (propargyl glycolide) polymer brushes have been successfully grown from Si/SiO_x. A post-polymerization "click" reaction to graft protein resistant functionality–oligo(ethylene glycol) to the polymer brush is reported. Preliminary protein resistance studies showed a large increase in the protein resistance lifetime of surfaces when oligo(ethylene glycol) is grafted to the polymer brushes. Finally, a Time of Flight–Secondary Ion Mass Spectroscopy study examining the grafting density as proceeding from the polymer brush air interface to the polymer brush surface interface is reported.

Oligo(ethylene glycol) Grafted Polyester Polymer Brushes as Dynamic Surfaces

by
Cameron Lee Stevens

A dissertation submitted to the Graduate Faculty of
North Carolina State University
in partial fulfillment of the
requirements for the degree of
Doctor of Philosophy

Chemistry

Raleigh, North Carolina
2018

APPROVED BY:

_____	_____
Christopher B. Gorman Committee Chair	Edmond Bowden
_____	_____
Jan Genzer	Joshua Pierce

DEDICATION

To my late father and nan who passed away at the beginning of my graduate studies.

BIOGRAPHY

Cameron L. Stevens grew up from humble beginnings in the foothills of the Allegheny mountains. First in his family to pursue a bachelor's degree; he graduated in 2013 from Juniata College. During his undergraduate career, he had the opportunity to train under Prof. Diane Nutbrown, Prof. I. David Reingold, and Prof. John B. Unger. On occasion, Cameron has recounted the sleepless nights spent in the depths of von Liebig Science Center learning the fundamentals of the Arts and Sciences. Through rigorous studies he was presented the opportunity to continue his education at North Carolina State University. Arriving in Raleigh in the fall of 2013 he began the next journey in his life under the supervision of Prof. Christopher B. Gorman. He departs this institution a better, more curious, and enlightened person.

ACKNOWLEDGMENTS

To my friends who have spent countless nights crowded around a small table discussing art, science, life, literature, anatomy, history, and everything in between. While we may never discover the true meanings of the topics spoken; those discussions brought us happiness in the moment. Our candid conversations, inside jokes, and nuanced lingo will forever hold a place in my heart. Sharing those times with you was priceless. To my mother and brother who have been supportive of me from afar. I would never have taken this journey without your guidance, support, and compassion.

I'd like to thank my lab mates who have been supportive of me throughout the past 5 years. An enormous thank you to my advisor Dr. Christopher Gorman for his guidance and encouragement throughout my studies. Finally, to you, the reader- I hope you find what you came looking for. I wish you happiness and prosperity in your future endeavors.

TABLE OF CONTENTS

LIST OF TABLES

LIST OF FIGURES

CHAPTER 1

Introduction

Biomaterials

Biomaterials are defined as "any natural or synthetic material (which includes polymer or metal) that is intended for introduction into living tissue especially as part of a medical device or implant"[1] Biomaterials have been used since antiquity. The first examples of biomaterials include tooth filling materials, wire to connect teeth, and wooden limb replacements. While the use of these archaic materials hardly constitute the modern definition of the word "biomaterials" they laid the ground work for modern scientists to explore how materials interact with the body.[2] Biomaterials have found a range of uses in implants[3], sensors[4], tissues scaffolds[5], drug delivery[6–8], dental repair[9], and wound healing.[10]

Modern medical devices also include a variety of biomaterials. These medical devices include a variety of implants, limb replacements, and monitors. Glucose sensors such as those developed by MEDCO© are the latest generation of medical devices that can continuously monitor glucose levels. These medical devices operate by measuring analytes within bodily fluid. These sensors allow patients to actively measure important analytes within their body and could allow for targeted dosing of medications. Despite the benefits of these sensors there remain several drawbacks. Most notably the replacement of the sensor in contact with bodily fluid. Currently, the best functioning sensors need to be replaced weekly.[11]

This problem of sensor replacement is not just limited to glucose sensors. Many artificial surfaces placed in contact with the body suffer from rejection, expulsion, or infection. To understand this phenomenon, one must first understand what happens when an artificial surface is placed into contact with bodily fluid. Upon contact with bodily fluids any surface will rapidly develop a hydration shell followed immediately by protein adsorption. Proteins

will adhere to almost any surface upon contact. Proteins can denature to cause a cascading series of events that can trigger an immune response to the surface. If bacteria are present or contact the surface they can cause rapid colonization and biofilm formation resulting in infections.[12] (Figure 1)

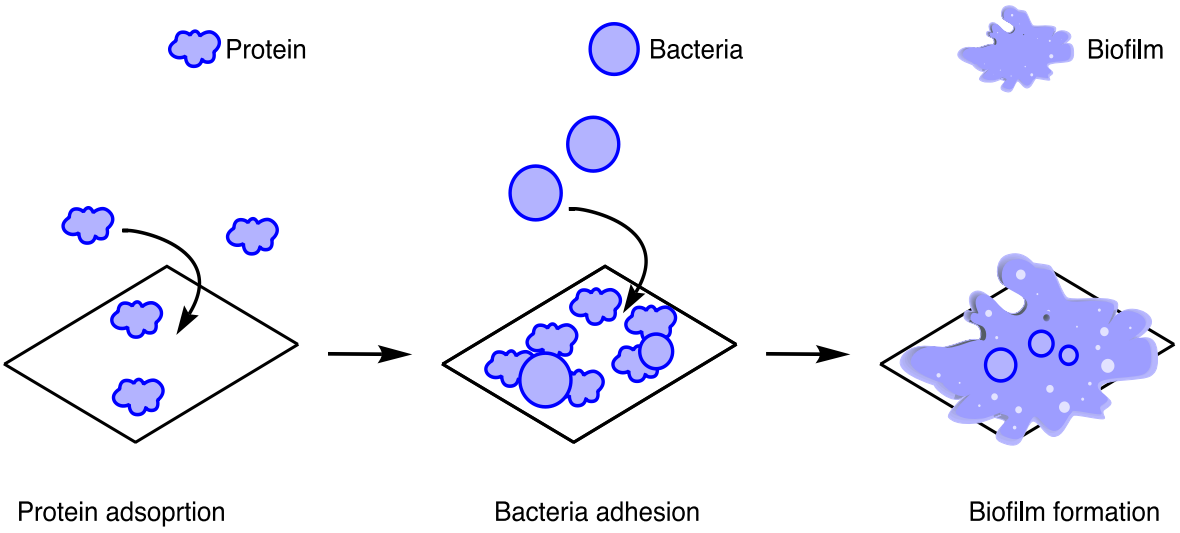

Figure 1 Cartoon representation of a surface in contact with bodily fluids over time.

To prevent or delay the rapid protein adsorption and subsequent onset of biofilm formation a variety of static surface coatings have been developed. These include hydrophobic,[12,13] zwitterionic,[14,15] cationic,[16–18] and biomolecular tethered surfaces[12,19–21] Currently, the "gold standard" for resisting biofouling in medical devices is poly(ethylene glycol) (PEG).[22] PEG coatings help facilitate the formation of a hydration layer around the device. This hydration layer has been attributed to PEG's observed protein resistance. However, all static surfaces will eventually foul with proteins, thus a dynamic or smart surface with integrated protein resistant functionalities is needed.

Dynamic surfaces

Borne of nature's ability to selectively tailor molecular assemblies and interfaces to provide specific, precise molecular interactions, dynamic surfaces, stimuli-responsive surfaces, or smart surfaces have become an increasingly large area of study. This emerging class of surface materials have the ability to change surface properties in response to a stimulus (e.g., force, pH, temperature, solvent, light).[23–27] Applications of these surfaces include dynamic control of biomolecule/surface interactions, complex self-assembly processes on surfaces, data storage devices, as well as a host of other applications.[26,27] Some examples of dynamic surfaces include thin films, self-assembled monolayers (SAMs), and polymer brushes.

Thin films

Thin films can broadly be defined as a film of material less than a few microns thick, deposited on a substrate. For practical purposes the discussion of thin films here will only concern organic or polymeric thin films. Thin films are important for modern technologies because they allow for control of surface structure property relationships. Additionally, thin films have been used to study interfacial phenomenon,[28] protein adsorption,[28] and adhesion.[29,30] There are a variety of deposition methods used to create thin films. These include: drop coating, spin coating, and dip coating. The deposition method of the film can create vastly different properties and thicknesses. Creation of thin films presents an opportunity to introduce unique functionalities and properties that a bulk substrate may lack. These include introducing conducive films for circuits,[22] attenuated wetting properties,[22] and imparting resistance to biological systems for medical devices.[31,32]

Although many unique surface properties have been developed through the study of thin films there remain limitations. Thin films are frequently deposited to a substrate via

solution creating potential complications in solubility. Modern solution processing methods create limited order in the system. The characterization and irreproducibility of thin films can also cause problems when scaling these systems to an industrial scale. Additionally, complications can arise when the films delaminate under stress.[28]

Self-assembled monolayers

Self-assembled monolayers (SAMs) are a class of molecular assemblies that can be used to make dynamic surfaces. SAMs often consist of a head group that binds to a surface, a tail that points away from the surface, and an end group that can be used as an anchoring point for additional functionality (Figure 2).[33] SAMs form, in part, because of the high affinity of their head group with the substrate. SAMs have been used extensively to study interfacial phenomena including wetting,[34] adhesion,[35] and protein resistance.[36]

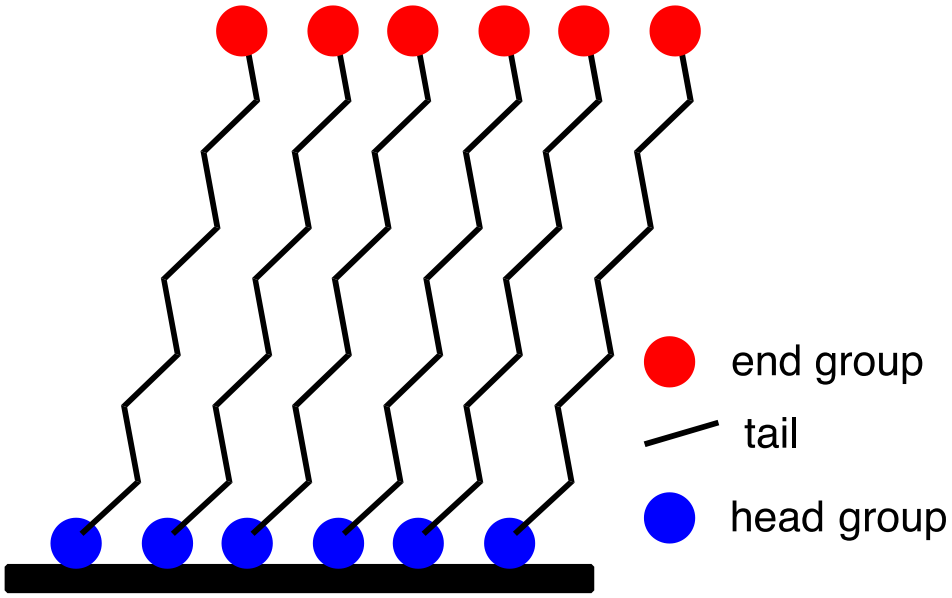

Figure 2: Cartoon representation of self-assembled monolayer on a surface

Polymer brushes

Another major class of stimuli-responsive surfaces are polymer brushes. Much like SAMs, polymer brushes consist of an anchoring group followed by a regular repeating structure from the surface. Polymer brushes of homopolymers, copolymers, and block copolymers have been prepared (**Figure 3**).[37] Polymer brushes are made via polymerization from or grafting to the surface. For example, polyelectrolyte brushes can respond to the ionic strength of solutions with large conformational changes. Additionally, architectural features (i.e., grafting density, thickness, length) of polymer brushes can be controlled and modified.[37]

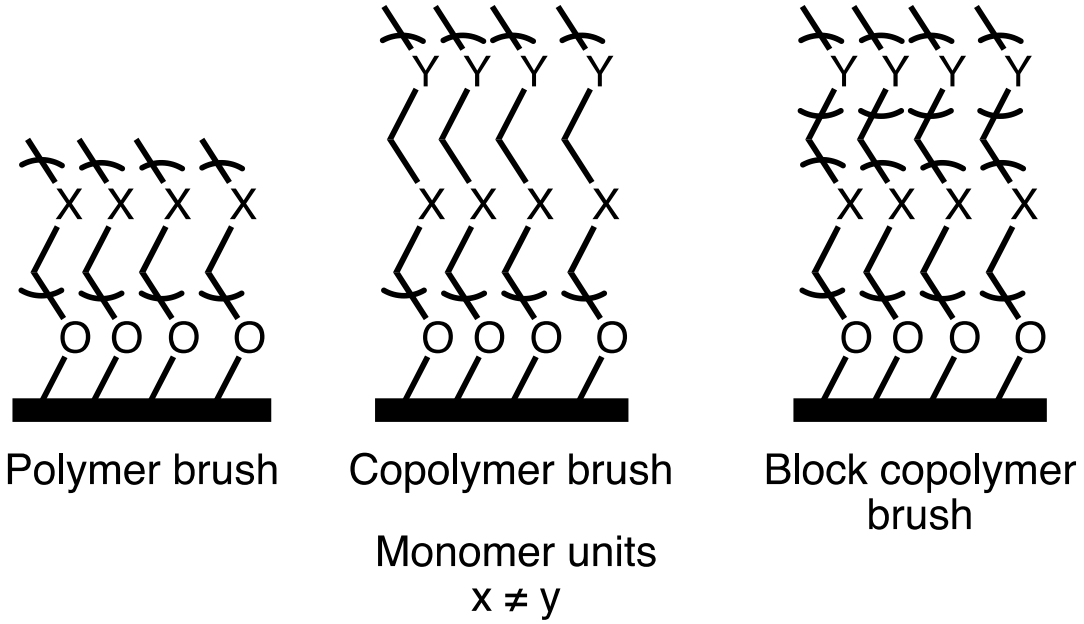

Figure 3: Cartoon representation of a homopolymer, copolymer, and block copolymer brushes on a surface

Polymer brushes can be made via the "grafting to" method. This involves grafting polymers in a solution to a substrate. For example, reversible addition-fragmentation chain-transfer polymerization can be used to produce poly (methacrylate) brushes. "Grafting through" is another method for making polymer brushes. The grafting through method involves polymerization in the presence of a monomer that is similar to a substrate-bound functional group. The polymerization of styrene in the presence of methyacrylate end capped poly(lactide) is one example of the grafting through method.[38] The "grafting from" method is the most commonly used method for making polymer brushes. In this method, surface substrate moieties are utilized as initiators in the polymerization of monomers in solution. For instance, ring opening polymerization can be initiated by taking advantage of the OH functional groups on silica.[39]

Polymer brushes can adopt a range of confirmations based on grafting density. Grafting density is defined as the number of polymer chains/ unit area. Lower grafting densities result

in surfaces that are considered to be in the "mushroom regime", while higher grafting densities lead to extended chains in the "brush regime". [28,40] Attenuating grafting density can lead to different properties of the surface.

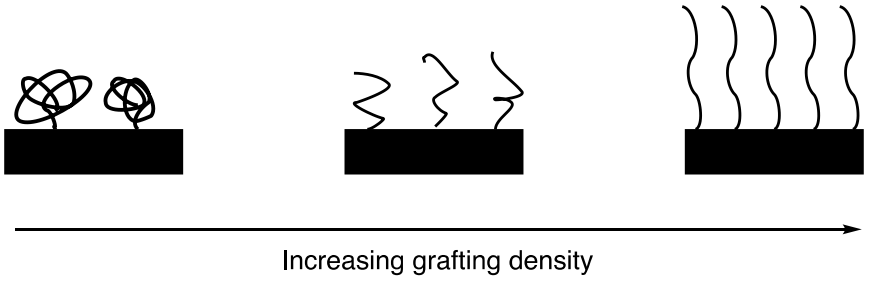

Figure 4: Cartoon representation of polymer brush regimes

Thin films, SAMs and polymer brushes create mediums between substrates and interfaces that allow for attenuating properties. These properties include converting a hydrophilic surface to a hydrophobic surface,[41] and coating metal substrates with organic functionalities.[33] One prominent example of this unique property modification is the use of SAMs to resist protein adsorption on surfaces that rapidly adsorb protein.[42]

Previous work

Some of the first work on creating protein resistant surfaces was developed by Prime and Whitesides.[43] They deposited SAMs on gold utilizing thiol head groups and oligo(ethylene glycol) (OEG) end groups. It was shown that the use of OEG reduced the protein adsorption and the incorporation of more hydrophobic groups increased protein adsorption. This seminal work has helped to guide the use of SAMs for protein resistant coatings.

Kankate et al. have recently studied the protein resistance of oligo (ethylene glycol) terminated SAMs on gold. In their study, they used surface plasmon resonance to measure the adsorption of a flowing protein solution over vapor deposited SAMs. When compared to a gold

thin film standard, vapor deposited surfaces showed no significant BSA protein adsorption over the course two 8 minute intervals of exposure.[44]

Chilkoti and coworkers demonstrated the Poly (oligoethylene glycol) methyl methacrylate brushes grown from SAMs on gold did not adsorb any fibronectin after being in contact with it for 20 minutes. They also showed that cells could be patterned on their surfaces and limited growth was seen after 3 days. This work was among the first to demonstrate "non-fouling" polymer brushes by surface-initiated polymerization of a macromonomer.[45]

Protein resistant functionalities are not just limited to SAMs. Psarra et al. studied dodecyl end capped poly (N-isopropylacrylamide) (PNIPAM) brushes and native PNIPAM brushes to understand the physicochemical surface characteristics. They showed the that addition of the dodecyl chain to PNIPAM created a system that lost protein (fibronectin) resistance above the lower critical solution temperature when compared to native PNIPAM brushes.[46] This work is consistent with the established trend that proteins will rapidly adsorb to nonpolar substrates.

Jiang et al. have studied the effects of varying repeat length of oligo (ethylene glycol) on gold SAMs. In their recent work, they showed that the best surfaces for resisting protein adsorption possessed terminal oligo (ethylene glycol) chains of at least six repeat units. The packing density and hydration layer are suggested as major factors in reducing protein adsorption.[47]

Previously, the Gorman group has shown that poly (lactic acid) (PLA) brushes can be grown via ring opening polymerization (ROP) of lactide using surface hydroxyl groups as initiators and $Sn(Oct)_2$ as a catalyst. PLA brushes have been grown from silicon surfaces and hydroxy terminated self-assembled monolayers (SAMs) on gold surfaces. Polymer brushes up

to 100 Å in thickness have been prepared and characterized.[39] These polymer brushes have the built in functionality that they are degradable. It was initially theorized that the act of degradation could reduce protein adsorption so they undertook further studies to understand the brush degradation mechanisms.

Studying the effects of pH and temperature on the degradability of PLA brushes showed that they can greatly influence the degradation kinetics. PLA brushes exposed to basic phosphate buffers (pH = 8) degraded much more rapidly than brushes in acidic buffers (pH = 6) (**Figure 5**). It is worth noting that this degradation is different from bulk PLA, which degrades under both acidic and basic pH conditions. PLA brushes also degrade much faster at elevated temperature (60 °C), then brushes incubated at lower temperatures (Figure 5)

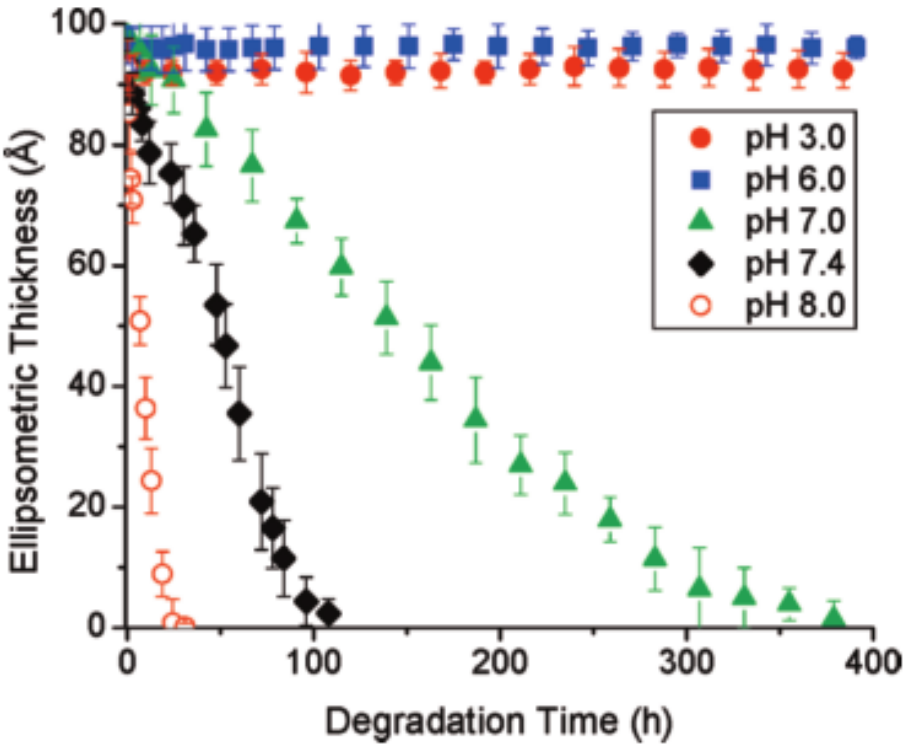

Figure 5: Degradation of PLA at varying pH. Reproduced from reference: 48

In addition to PLA, poly(ε-caprolactone) (PCL) and poly(glycolic acid) (PGA) brushes have also been grown from surfaces. Again, it was theorized that the act of degradation of these brushes could be used as a dynamic surface to resist protein adsorption. Initial studies showed that significant amounts of protein aggregated to the polyester brushes in under 30 hours. Block copolymer brushes with oligo(ethylene glycol) (OEG) were synthesized and showed better protein resistance. In one case, Si-OEG-PGA block copolymers were relatively protein resistant for 3 days (Figure 6).[49]

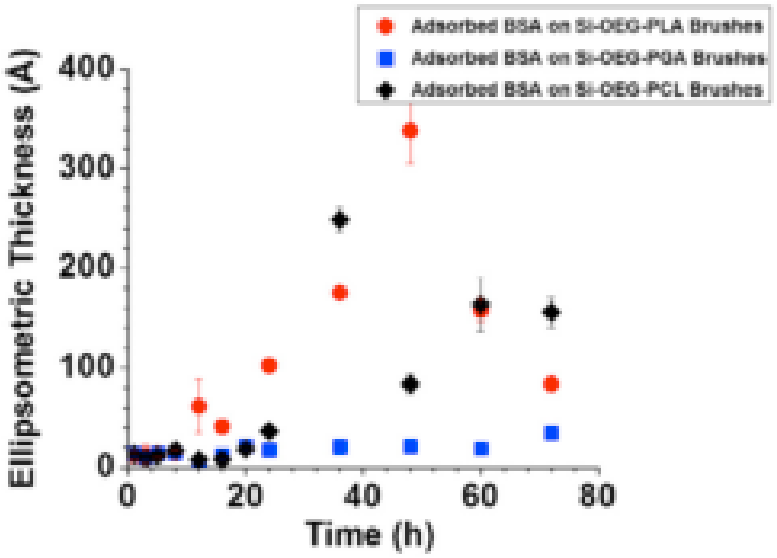

Figure 6: Plot of adsorbed bovine serum albumin (BSA) on Si-OEG-PLA, Si-OEG-PGA, Si-OEG-PCL brushes. Reproduced from reference 49.

Given the success of OEG incorporation into polyester brushes, it was hypothesized that incorporation of OEG side chains into the monomers might produce a more "PEG-like" surface and thus give additional protein resistance, while still being degradable through the backbiting mechanism proposed in poly(lactide) (Figure 7).[50]

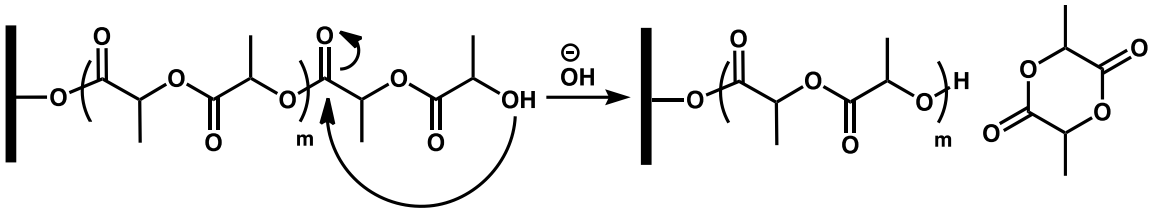

Figure 7: Proposed backbiting mechanism of polyester brush

Research Goals

The goal of this project is to develop a protein resistant surface that is also dynamic (Figure 8). All static surfaces will eventually foul when exposed to protein, by creating a polymer brush

that is both resistant to protein and degradable when proteins adsorb, a non-fouling dynamic surface could be created. These thin films could be used to give surfaces longer lifetimes *in vivo*. To accomplish this goal two methods have been explored:

1) The synthesis of a novel monomer with OEG appended side chains. This approach would allow us to explore the feasibility of surface initiated polymerization (SIP) with new monomers and would allow for incorporation of OEG into each monomer unit.
2) The synthesis of a monomer containing a cyclic diester functionality that has been previously used to grow polymer brushes but would have additional motifs that would allow for post polymerization modification.

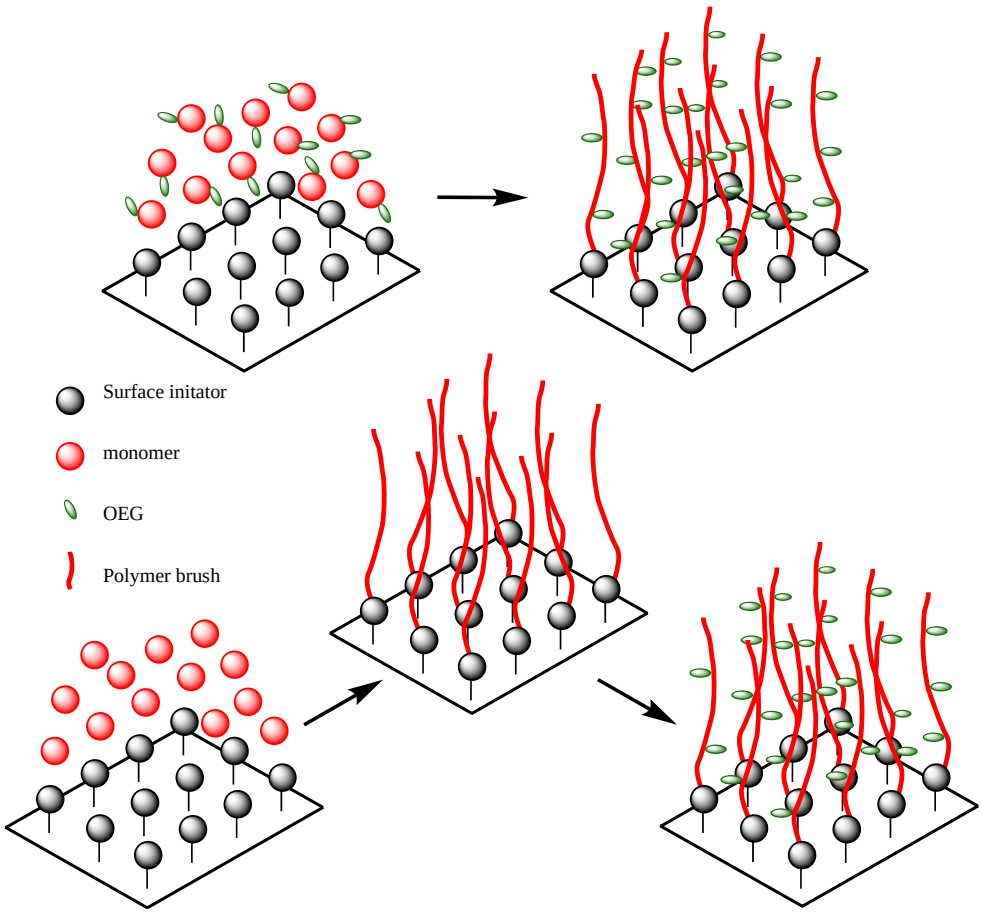

Figure 8: Cartoon representation of different methods for making polymer. Top novel monomer with OEG side chains bottom PPM of polymer brushes

References

(1) Bhat, S.; Kumar, A. Biomaterials and Bioengineering Tomorrow's Healthcare. *Biomatter* **2013**, *3* (3).

(2) Migonney, V. History of Biomaterials. In *Biomaterials*; John Wiley & Sons, Inc.: Hoboken, NJ, USA, 2014; pp 1–10.

(3) Roach, P.; Eglin, D.; Rohde, K.; Perry, C. C. Modern Biomaterials: A Review - Bulk Properties and Implications of Surface Modifications. *J. Mater. Sci. Mater. Med.* **2007**, *18* (7), 1263–1277.

(4) Mohanty, S. P.; Kougianos, E. Biosensors: A Tutorial Review. *IEEE Potentials* **2006**, *25* (2), 35–40.

(5) Vats, A.; Tolley, N. S.; Polak, J. M.; Gough, J. E. Scaffolds and Biomaterials for Tissue Engineering: A Review of Clinical Applications. *Clin. Otolaryngol. Allied Sci.* **2003**, *28* (3), 165–172.

(6) Langer, R.; Peppas, N. A. Advances in Biomaterials, Drug Delivery, and Bionanotechnology. *AIChE J.* **2003**, *49* (12), 2990–3006.

(7) Langer, R.; Peppas, N. Present and Future Applications of Biomaterials in Controlled Drug Delivery Systems. *Biomaterials* **1981**, *2* (4), 201–214.

(8) Langer, R. Biomaterials in Drug Delivery and Tissue Engineering: One Laboratory's Experience. *Acc. Chem. Res.* **2000**, *33* (2), 94–101.

(9) Nicholson, J. W. Adhesive Dental Materials—A Review. *Int. J. Adhes. Adhes.* **1998**, *18* (4), 229–236.

(10) Boateng, J. S.; Matthews, K. H.; Stevens, H. N. E.; Eccleston, G. M. Wound Healing Dressings and Drug Delivery Systems: A Review. *J. Pharm. Sci.* **2008**, *97* (8), 2892–2923.

(11) Wang, H. C.; Lee, A. R. Recent Developments in Blood Glucose Sensors. *J. Food Drug Anal.* **2015**, *23* (2), 191–200.

(12) Harding, J. L.; Reynolds, M. M. Combating Medical Device Fouling. *Trends Biotechnol.* **2014**, *32* (3), 140–146.

(13) Epstein, A. K.; Wong, T.-S.; Belisle, R. A.; Boggs, E. M.; Aizenberg, J. Liquid-Infused Structured Surfaces with Exceptional Anti-Biofouling Performance. *Proc. Natl. Acad. Sci.* **2012**, *109* (33), 13182–13187.

(14) Siedenbiedel, F.; Tiller, J. C. Antimicrobial Polymers in Solution and on Surfaces: Overview and Functional Principles. *Polymers (Basel).* **2012**, *4* (1), 46–71.

(15) Jiang, S.; Cao, Z. Ultralow-Fouling, Functionalizable, and Hydrolyzable Zwitterionic Materials and Their Derivatives for Biological Applications. *Adv. Mater.* **2010**, *22* (9), 920–932.

(16) Zou, P.; Hartleb, W.; Lienkamp, K. It Takes Walls and Knights to Defend a Castle - Synthesis of Surface Coatings from Antimicrobial and Antibiofouling Polymers. *J. Mater. Chem.* **2012**, *22* (37), 19579–19589.

(17) Rabea, E. I.; Badawy, M. E. T.; Stevens, C. V.; Smagghe, G.; Steurbaut, W. Chitosan as Antimicrobial Agent: Applications and Mode of Action. *Biomacromolecules* **2003**, *4* (6), 1457–1465.

(18) Jayakumar, R.; Prabaharan, M.; Nair, S. V.; Tamura, H. Novel Chitin and Chitosan Nanofibers in Biomedical Applications. *Biotechnol. Adv.* **2010**, *28* (1), 142–150.

(19) Forbes, S.; McBain, A. J.; Felton-Smith, S.; Jowitt, T. A.; Birchenough, H. L.; Dobson, C. B. Comparative Surface Antimicrobial Properties of Synthetic Biocides and Novel Human Apolipoprotein E Derived Antimicrobial Peptides. *Biomaterials* **2013**, *34* (22),

5453–5464.

(20) Bilek, M. M. M.; Bax, D. V; Kondyurin, A.; Yin, Y.; Nosworthy, N. J.; Fisher, K.; Waterhouse, A.; Weiss, A. S.; dos Remedios, C. G.; McKenzie, D. R. Free Radical Functionalization of Surfaces to Prevent Adverse Responses to Biomedical Devices. *Proc. Natl. Acad. Sci.* **2011**, *108* (35), 14405–14410.

(21) Bazaka, K.; Jacob, M. V.; Crawford, R. J.; Ivanova, E. P. Plasma-Assisted Surface Modification of Organic Biopolymers to Prevent Bacterial Attachment. *Acta Biomater.* **2011**, *7* (5), 2015–2028.

(22) Konradi, R.; Acikgoz, C.; Textor, M. Polyoxazolines for Nonfouling Surface Coatings–a Direct Comparison to the Gold Standard PEG. *Macromol. Rapid Commun.* **2012**, *33* (19), 1663–1676.

(23) Lee, H.; Pietrasik, J.; Sheiko, S. S.; Matyjaszewski, K. Stimuli-Responsive Molecular Brushes. *Prog. Polym. Sci.* **2010**, *35* (1–2), 24–44.

(24) Jeong, B.; Gutowska, A. Lessons from Nature: Stimuli-Responsive Polymers and Their Biomedical Applications. *Trends Biotechnol.* **2002**, *20* (7), 305–311.

(25) Mano, J. F. Stimuli-Responsive Polymeric Systems for Biomedical Applications. *Adv. Eng. Mater.* **2008**, *10* (6), 515–527.

(26) Stuart, M. A. C.; Huck, W. T. S.; Genzer, J.; Müller, M.; Ober, C.; Stamm, M.; Sukhorukov, G. B.; Szleifer, I.; Tsukruk, V. V; Urban, M.; et al. Emerging Applications of Stimuli-Responsive Polymer Materials. *Nat. Mater.* **2010**, *9* (2), 101–113.

(27) Mendes, P. M. Stimuli-Responsive Surfaces for Bio-Applications. *Chem. Soc. Rev.* **2008**, *37* (11), 2512–2529.

(28) Wu, T.; Efimenko, K.; Vlček, P.; Šubr, V.; Genzer, J. Formation and Properties of

Anchored Polymers with a Gradual Variation of Grafting Densities on Flat Substrates. *Macromolecules* **2003**, *36* (7), 2448–2453.

(29) Hegemann, D.; Brunner, H.; Oehr, C. Plasma Treatment of Polymers for Surface and Adhesion Improvement. *Nucl. Instruments Methods Phys. Res. Sect. B Beam Interact. with Mater. Atoms* **2003**, *208* (1–4), 281–286.

(30) Litteken, C. S.; Dauskardt, R. H. Adhesion of Polymer Thin-Films and Patterned Lines. *Int. J. Fract.* **2003**, *119/120* (4–2), 475–485.

(31) Fu, J.; Ji, J.; Yuan, W.; Shen, J. Construction of Anti-Adhesive and Antibacterial Multilayer Films via Layer-by-Layer Assembly of Heparin and Chitosan. *Biomaterials* **2005**, *26* (33), 6684–6692.

(32) Adiga, S. P.; Jin, C.; Curtiss, L. A.; Monteiro-Riviere, N. A.; Narayan, R. J. Nanoporous Membranes for Medical and Biological Applications. *Wiley Interdiscip. Rev. Nanomedicine Nanobiotechnology* **2009**, *1* (5), 568–581.

(33) Love, J. C.; Estroff, L. A.; Kriebel, J. K.; Nuzzo, R. G.; Whitesides, G. M. Self-Assembled Monolayers of Thiolates on Metals as a Form of Nanotechnology. *Chem. Rev.* **2005**, *105* (4), 1103–1169.

(34) Abbott, N. L.; Gorman, C. B.; Whitesides, G. M. Active Control of Wetting Using Applied Electrical Potentials and Self-Assembled Monolayers. *Langmuir* **1995**, *11* (1), 16–18.

(35) Arima, Y.; Iwata, H. Effect of Wettability and Surface Functional Groups on Protein Adsorption and Cell Adhesion Using Well-Defined Mixed Self-Assembled Monolayers. *Biomaterials* **2007**, *28* (20), 3074–3082.

(36) DiMilla, P. A.; Folkers, J. P.; Biebuyck, H. A.; Harter, R.; Lopez, G. P.; Whitesides, G.

M. Wetting and Protein Adsorption on Self-Assembled Monolayers of Alkanethiolates Supported on Transparent Films of Gold. *J. Am. Chem. Soc.* **1994**, *116* (5), 2225–2226.

(37) Krishnamoorthy, M.; Hakobyan, S.; Ramstedt, M.; Gautrot, J. E. Surface-Initiated Polymer Brushes in the Biomedical Field: Applications in Membrane Science, Biosensing, Cell Culture, Regenerative Medicine and Antibacterial Coatings. *Chem. Rev.* **2014**, *114* (21), 10976–11026.

(38) Hawker, C. J.; Mecerreyes, D.; Elce, E.; Dao, J.; Hedrick, J. L.; Barakat, I.; Dubois, P.; Jérôme, R.; Volksen, W. "Living" Free Radical Polymerization of Macromonomers: Preparation of Well Defined Graft Copolymers. *Macromol. Chem. Phys.* **1997**, *198* (1), 155–166.

(39) Xu, L.; Gorman, C. B. Poly(Lactic Acid) Brushes Grow Longer at Lower Temperatures. *J. Polym. Sci. Part A Polym. Chem.* **2010**, *48* (15), 3362–3367.

(40) Wu, T.; Efimenko, K.; Genzer, J. Combinatorial Study of the Mushroom-to-Brush Crossover in Surface Anchored Polyacrylamide. *J. Am. Chem. Soc.* **2002**, *124* (32), 9394–9395.

(41) Howarter, J. A.; Youngblood, J. P. Self-Cleaning and Anti-Fog Surfaces via Stimuli-Responsive Polymer Brushes. *Adv. Mater.* **2007**, *19* (22), 3838–3843.

(42) Prime, K. L.; Whitesides, G. M. Adsorption of Proteins onto Surfaces Containing End-Attached Oligo(Ethylene Oxide): A Model System Using Self-Assembled Monolayers. *J. Am. Chem. Soc.* **1993**, *115* (23), 10714–10721.

(43) Prime, K. L.; Whitesides, G. M. Self-Assembled Organic Monolayers: Model Systems for Studying Adsorption of Proteins at Surfaces. *Science (80).* **1991**, *252* (5009), 1164–1167.

(44) Kankate, L.; Werner, U.; Turchanin, A.; Gölzhäuser, A.; Großmann, H.; Tampé, R. Protein Resistant Oligo(Ethylene Glycol) Terminated Self-Assembled Monolayers of Thiols on Gold by Vapor Deposition in Vacuum. *Biointerphases* **2010**, *5* (2), 30–36.

(45) Ma, H.; Hyun, J.; Stiller, P.; Chilkoti, A. "Non-Fouling" Oligo(Ethylene Glycol)-Functionalized Polymer Brushes Synthesized by Surface-Initiated Atom Transfer Radical Polymerization. *Adv. Mater.* **2004**, *16* (4), 338–341.

(46) Psarra, E.; König, U.; Ueda, Y.; Bellmann, C.; Janke, A.; Bittrich, E.; Eichhorn, K. J.; Uhlmann, P. Nanostructured Biointerfaces: Nanoarchitectonics of Thermoresponsive Polymer Brushes Impact Protein Adsorption and Cell Adhesion. *ACS Appl. Mater. Interfaces* **2015**, *7* (23), 12516–12529.

(47) Li, L.; Chen, S.; Zheng, J.; Ratner, B. D.; Jiang, S. Protein Adsorption on Oligo(Ethylene Glycol)-Terminated Alkanethiolate Self-Assembled Monolayers: The Molecular Basis for Nonfouling Behavior. *J. Phys. Chem. B* **2005**, *109* (7), 2934–2941.

(48) Xu, L.; Crawford, K.; Gorman, C. B. Effects of Temperature and PH on the Degradation of Poly(Lactic Acid) Brushes. *Macromolecules* **2011**, *44* (12), 4777–4782.

(49) Hu, X.; Gorman, C. B. Resisting Protein Adsorption on Biodegradable Polyester Brushes. *Acta Biomater.* **2014**, *10* (8), 3497–3504.

(50) Hu, X.; Hu, G.; Crawford, K.; Gorman, C. B. Comparison of the Growth and Degradation of Poly(Glycolic Acid) and Poly(ε-Caprolactone) Brushes. *J. Polym. Sci. Part A Polym. Chem.* **2013**, *51* (21), 4643–4649.

Chapter 2

Introduction

Poly (α-hydroxy acids) (PAHAs) are sought after for their biodegradability and thermoplastic properties.[1–3] The most commonly found PAHAs are those derived from PLA, and PGA. These polyesters are typically prepared using ring opening polymerization (ROP) of cyclic dimers of the corresponding α-hydroxy acid (Figure 9) Different catalysts and conditions have been investigated to control molar mass distribution, chain ends, and composition.[4–8] Despite these advances their remains limited structural diversity in PAHAs.[9,10]

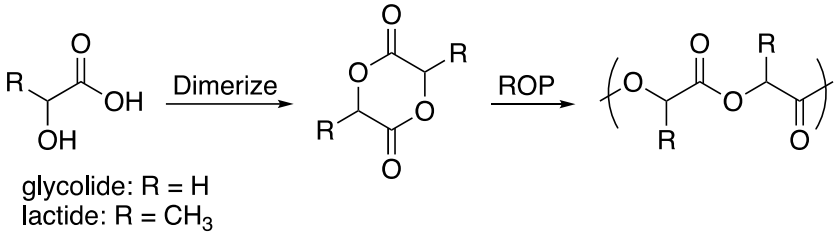

Figure 9: Dimerization and ring-opening polymerization of α-hydroxy acid

The limited structural diversity of PAHAs can be partially attributed to the difficulty of synthesizing monomers. The dimerization of α-hydroxy acids is typically catalyzed in the presence of an acid. An equilibrium exists between the formation of the cyclic monomer and polymerization of the α-hydroxy acid. Typical procedures will take advantage of the volatility of the monomer compared to the oligomers and starting material to distill out the desired product, this usually results in yields of <50%. The synthetically intensive nature of working with unsymmetrical dimers (often multiple steps and difficult purifications) of α-hydroxy acids also limit structural diversity.

Cyclic diester dimers with various pendant side chains are not easy to synthesize because of the equilibrium discussed above. The lack of commercially available α-hydroxy acids to dimerize may also play a role in the narrow window of monomer scope. Thus,

alternative methods are needed both in structural diversity of α-hydroxy acids as well as new ways to form poly (α-hydroxy acids).

Recently, alternatives to the dimerized α-hydroxy acids have become popular. The *O*-carboxy anhydride functionality has been studied to convert substituted α-hydroxy acids into viable monomers for polymerization.[11] The use of this functionality eliminates one of the major problems with dimerization of α-hydroxy acids- it does not require the product to be volatile.[12]

Results and Discussion

Development of monomers with oligoethylene glycol side chains.

A few routes have been developed to produce cyclic diester monomers with OEG side chains. Rubinshtein et al synthesized a nonsymmetrical hemilactide by a Passerini-type condensation that featured an azide terminated OEG side chain.[13] Baker synthesized a OEG/alkyl asymmetric cyclic diester in low yields (<15%) that could be converted into bottle brushes.[14] PEG-grafted caprolactone monomers like that developed by Jérôme have also been synthesized.[15] However, none of these routes are high yielding and they all lack generality. A new approach which is more modular could help to increase the structural diversity of PAHAs as well as generate different derivative side chains.

Proposed new monomer with an OEG side chain

W. H. Davie first reported the synthesis of anhydro-*O*-carboxy glycolic acid in 1951 by treatment of glycolic acid with phosgene (carbonyl chloride).[16] Since that time, molecules with this functionality have seen modest use in controlled polymerizations.[11,17,18] The synthesis of various derivatives of the anhydro-*O*-carboxy or *O*-carboxy anhydride (OCA) moiety remain challenging due to their highly reactive nature.[12] A literature review lead to only a few

examples of PAHAs made from ring opening polymerization (ROP) of substituted O-carboxy anhydrides (OCA).[19–21]

It is of interest to explore new side chain functionalities of the OCA moiety. One potentially interesting functionality lacking is the incorporation of ethylene glycol into the monomer. Oligo(ethylene glycol) (OEG) or Poly(ethylene glycol) (PEG) are commonly used in biomaterials to limit protein adsorption on hydrophobic functionalities.[22] Functionalization of OCA with an OEG side chain could allow for ROP to provide a new class of biomaterials.

Synthesis of hydroxyl-appended OCA

A review of the literature led to a report from Cheng *et al.* that a benzyl protected OCA (**3**) could be prepared using readily available benzyl protected serine (**1**). This monomer was subsequently polymerized under mild conditions.[23] Deprotection of the polymer allowed for post-polymerization modification (PPM). It is proposed that this (**3**) compound could be a useful starting material for an OEG-appended OCA monomer (**5**).

Scheme 1: Proposed synthetic route to OEG-OCA

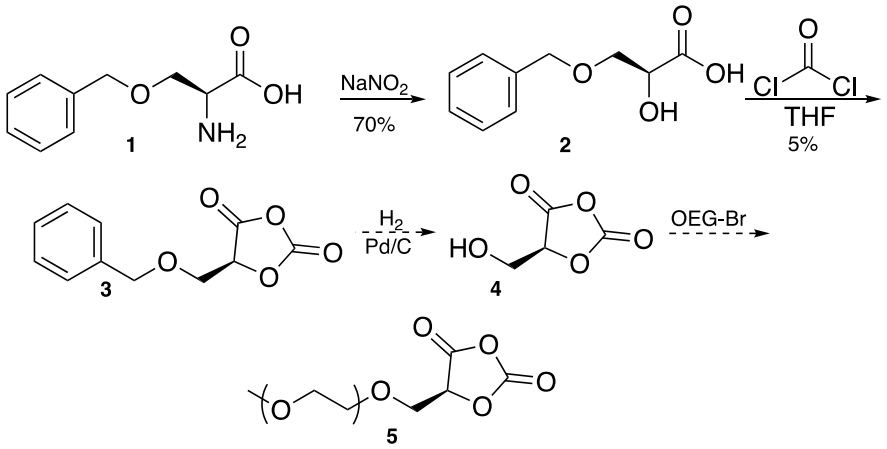

A first attempt to develop a synthetic route to prepare OEG-OCA (**5**) is shown in Scheme 1. Treatment of benzyl protected serine (**1**) with $NaNO_2$ produced the corresponding

α-hydroxy acid (**2**) in 70% yield. Treatment of α-hydroxy acid with phosgene at room temperature produced the corresponding OCA in low yield.[16] The low yields of this monomer may be attributed to the difficulty in purification. Demings et al. showed that the difficulties involved in the synthesis of (**3**) could have been caused by the grade and moisture content of the silica used during purification.[24] Further complications arose when deprotection of the monomer (**3 → 4)** led to a mixture of polymer and side products that could not be identified by ^{1}H NMR. It is hypothesized that the alcohol moiety on the deprotected monomer (**4**) acted as an initiator to promote ring opening of the OCA. Isolation of the hydroxyl-OCA (**4)** was not achieved.

Attempted synthesis of OEG-appended OCA

Rather than employ a complex synthetic route utilizing benzyl protected serine a more direct route to OEG-appended, α-hydroxy acid (**9)** was explored (Scheme 2). A review of the literature related to the synthesis of α-hydroxy acids led to a route starting from 3-chloro-2-hydroxypropanoic acid (**6)**.[25,26] It was hypothesized that this compound could be reacted with a nucleophile to substitute an oligoethylene glycol (OEG) moiety at the 3 position. Cyclization could then be achieved with phosgene, or a similar reagent, to generate a oligoethylene glycol-appended *O*-carboxyanhydride (OEG-OCA, **9**).

Scheme 2: Proposed synthesis of OEG-appended OCA

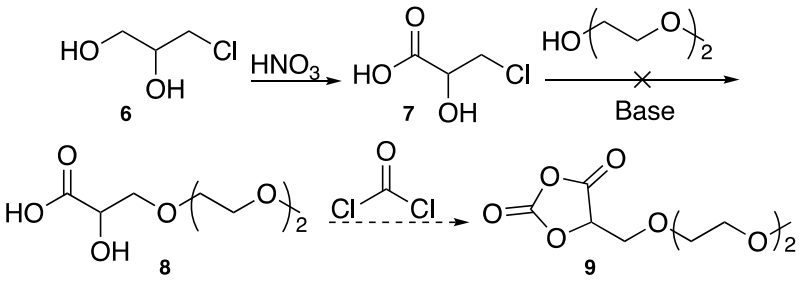

To pursue the synthesis outlined in Scheme 2, 3-chloro-2-hydroxypropanoic acid (**7)** was prepared as described in the literature via a biphasic reaction using concentrated nitric acid to oxidize 3-chloropropane-1,2-diol to the corresponding acid (**7**).[25] Removal of over oxidized products (i.e., oxalic acid) could be achieved via treatment with $CaCO_3$. After sublimation, white crystals were recovered in 21% yield.

A solution of potassium 2-(2-methoxyethoxy)ethan-1-olate (K-DEG) was prepared by dripping diethylene glycol monomethyl ether into a slurry of potassium metal and THF. Attempts to treat 3-chloro-2-hydroxypropanoic acid (**7)** with K-DEG under S_N2 conditions yielded no desired product as evidenced by NMR. Attempts to do an *in situ* Finkelstein reaction by treating 3-chloro-2-hydroxypropanoic acid (**7)** with NaI were also unsuccessful.

Given the difficulty of reacting K-DEG with the beta chlorine, alternative routes were explored. It had been reported that 3-chloro-2-hydroxypropanoic acid (**7)** could be converted to the corresponding epoxide (**10**) via KOH (Scheme 3).[26] Preparation of the corresponding epoxide was completed in 32% yield. Attempts to open the epoxide were unsuccessful using basic epoxide ring opening procedures. It was hypothesized that this result might be due to the poor solubility of the epoxide in organic solvents. To circumvent this problem attempts were made to protonate the carboxylate (**10**). It was reasoned that the protonated carboxylic acid would be more soluble in organic solvents than the potassium carboxylate salt (**10**). However,

when the potassium carboxylate salt was treated with various protic acids (HNO_3 and H_2SO_4), elimination to form acrylic acid competed with protonation of the carboxylate salt (**17)**, as evidenced by crude ^1H NMR.

Scheme 3: Proposed synthetic route to OEG-α-hydroxy acid salt

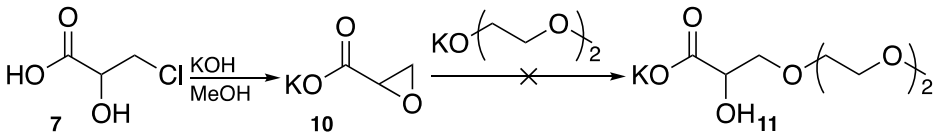

Given the difficulty of working with K-DEG and the carboxylic acid functionality, a new substrate was sought. It was hypothesized that utilizing an ester instead of an acid would increase stability and solubility in organic solvents. Thus, the reaction sequence shown in Scheme 4 was pursued.

Methyl oxirane-2-carboxylate (**13)** was prepared in large quantities via a biphasic reaction of commercial bleach and methyl acrylate (**12)** as described in the literature.[27] After distillation, a colorless oil was isolated in 45% yield.

Attempts were made to open the epoxide via S_N2 conditions using methoxide as a nucleophile; however, no desired product was isolated. Several Lewis acids were surveyed as catalysts for the ring opening of methyl glycidate (**13**) including $LiClO_4$, $ZnCl_2$, and $Sc(OTf)_2$. Ultimately, it was determined that $Mg(ClO_4)_2$ produced the ring opened product, 2-hydroxy-3-methoxypropanoic acid (**14)**, in good yields (80%). Use of TEG to ring open the epoxide produced the desired product, methyl 13-hydroxy-2,5,8,11-tetraoxatetradecan-14-oate (**15)**, in slightly lower yields (50%). Treatment of the ester with KOH in methanol yielded the corresponding acid, 13-hydroxy-2,5,8,11-tetraoxatetradecan-14-oic acid (**17)**, in moderate yields (54%).

Scheme 4: Proposed synthetic route to OEG-OCA

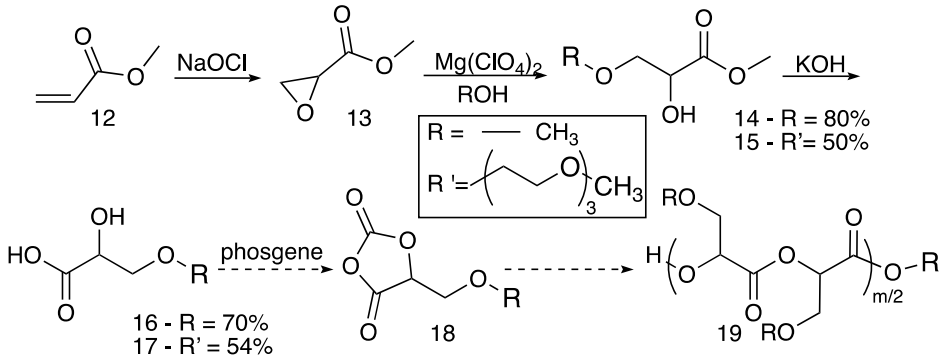

After saponification, it was envisioned that the acid could be cyclized to the corresponding OEG-OCA (**18**). 2-Hydroxy-3-methoxypropanoic acid (**16**) was used as a model compound for cyclization. Triphosgene and phosgene in solution were used to make MeOOCA (**18**, R = CH_3). ^{1}H NMR of the crude product showed resonances consistent with the desired product (Figure 9); however, isolation of the MeOOCA (**18**) was problematic. Distillation was attempted; however, heat resulted in ring opening as evidenced by ^{1}H NMR (not shown). Attempts at recrystallization yielded impure oils. Several attempts were made to purify the compound on silica gel, alumina, and reverse-phase silica. Deming *et al.* have reported purification of N-carboxyanhydrides using rigorously dried silica in a glove box.[27] This procedure was attempted, but, only mixtures of the product and an unknown impurity were isolated.

It was considered that the impure monomer might be appropriate for polymerization. However, Hu et al. reported that lactide ROP was unsuccessful with impure lactides.[28,29] Thus, it seemed important to test if minor impurities in the OCA system would hinder polymerizations. However, experiments to polymerize the crude OCA system using conditions previously reported for OCA polymerizations where unsuccessful.[30]

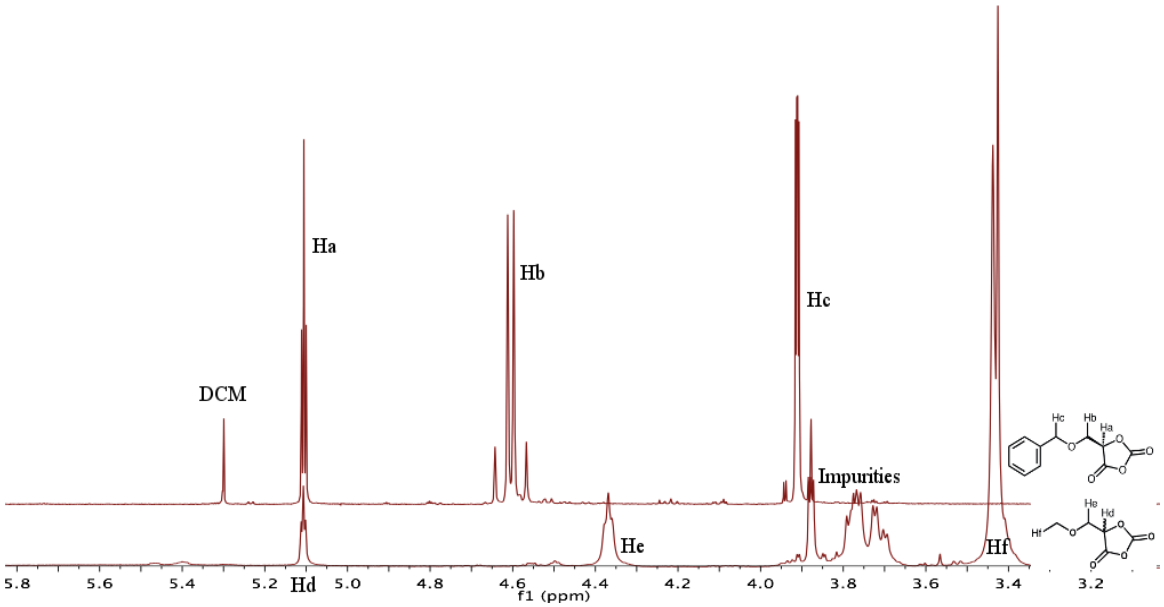

Figure 10: 1H NMR comparison of MeOOCA (18) and benzyl-protected OCA (3)

Attempted synthesis of polymer brushes using known OCA

After the isolation of the desired OCA could not be achieved, and crude mixtures did not yield any polymer it was still of interest to study if the OCA functionality could be used to create polymer brushes. To do this- it was hypothesized that known OCA derivatives could be synthesized and polymerization conditions on surfaces could be explored.

One of the most common OCA monomers studied is 5-phenyl-1,3-dioxolane-2,4-dione (**21**) this mandelic acid OCA is derived from carbonylation reaction of mandelic acid with diphosgene (Scheme 5). The mandelic acid OCA has been shown to undergo ring-opening polymerization (ROP) in the presence of a pyridine catalyst to give the corresponding PAHA.[30]

Scheme 5: Carbonylation reaction of mandelic acid with diphosgene to make 5-phenyl-1,3-dioxolane-2,4-dione

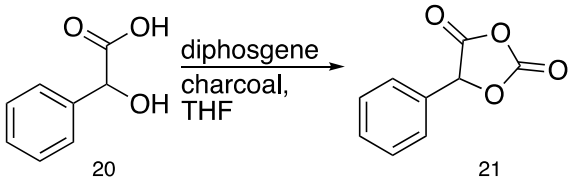

To test this hypothesis the mandelic acid-derived OCA (**21**) was polymerized using trace water as an initiator and pyridine as the catalyst in a sealed NMR tube to monitor polymerization. After 20 hours, the sharp methine peak at 6.08 ppm had completely disappeared and a broad multiplet at 6.10-5.95 had appeared. After confirming the polymerization reaction worked in solution experiments to test the feasibility of brush growth using this system were conducted.

Solutions of mandelic acid-derived OCA were placed over freshly clean silicon wafers with pyridine as a catalyst varying times, solvent, and temperature. In chloroform at room temperature brush thickness measured by ellipsometry decreased at longer reaction times These data are entries 1-3 of Table 1. At 24 hours, the poly mandelic acid brush was 4.0 nm thick compared to a value of 2.31 nm at 91 hours. At slightly elevated temperatures (40 °C) brush thickness increased slightly with longer reaction time this can be seen in entries 4 and 5 in Table 1. At higher temperatures, almost no brush growth was observed (1.5 nm at 50 °C). Attempts to use dichloromethane to grow brushes showed no growth or degradation for brushes at longer reaction times (entries 7-9 in Table 1). Increasing the temperature of polymerization in DCM gave slightly longer brushes (entries 10 and 11 in Table 1).

Attempts to polymerize 5-phenyl-1,3-dioxolane-2,4-dione from surfaces varying time temperature, and solvent resulted in minimal (< 5 nm) growth of brushes from wafers. Given this result, efforts to synthesize polymer brushes from other OCA derivatives were abandoned.

Table 1: Reaction conditions for attempted mandelic acid-derived OCA polymerization on silica

Entry	Time (h)	Temperature (°C)	Solvent	Thickness (nm)
1	24	RT	CH_3Cl	4.0 (0.31)
2	48	RT	CH_3Cl	3.07 (0.42)
3	91	RT	CH_3Cl	2.31 (0.44)
4	24	40	CH_3Cl	1.86 (0.32)
5	48	40	CH_3Cl	3.82(0.24)
6	24	50	CH_3Cl	1.5 (0.51)
7	48	RT	DCM	2.51 (0.47)
8	72	RT	DCM	2.48 (0.12)
9	141	RT	DCM	2.37 (0.21)
10	48	40	DCM	3.03 (0.54)
11	72	40	DCM	3.18 (0.36)

In conclusion, a new method to synthesize OEG-derivatives of α-hydroxy acids has been created, producing new molecules 2-hydroxy-3-methoxypropanoic (**16**) acid and 13-hydroxy-2,5,8,11-tetraoxatetradecan-14-oic acid (**17**). Additionally, 5-(methoxymethyl)-1,3-dioxolane-2,4-dione (**18**) has been synthesized albeit with impurities Attempts to use the impure OCA for polymerizations were unsuccessful. Attempts to polymerize a known OCA derivative from a surface using the native hydroxyl groups as initiators as a proof of concept showed only minimal growth of the polymer brush and no further growth over time. Given the difficulty in working with OCA-based monomers, other routes to OEG-functionalized polymer brushes were explored.

Experimental

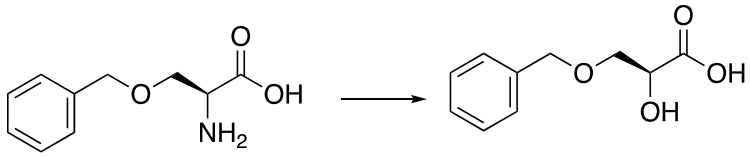

Synthesis of (S)-3-(benzyloxy)-2-hydroxypropanoic acid (**2**): Acetonitrile (64 mL) and 1 M sulfuric acid (64 mL) were added to *O*-benzyl-L-serine (4.9 g, 25 mmol) under nitrogen. In a separate flask, $NaNO_2$ (3.42 g, 51 mmol) was dissolved in water (25 mL), and then transferred to the *O*-benzyl-L-serine slurry while stirring under inert atmosphere. The reaction was allowed to stir at room temperature overnight. The aqueous layer was extracted with dichloromethane (DCM), dried over $MgSO_4$, and concentrated *in vacuo* to yield a yellow oil (3.5 g, 70% yield). ^{1}H NMR matched that reported previously.[20]

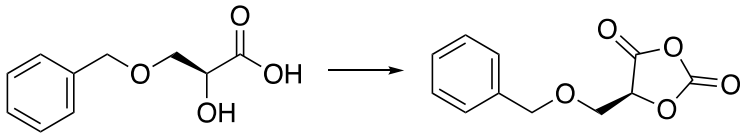

Synthesis of 5-((benzyloxy)methyl)-1,3-dioxolane-2,4-dione (**3**): Triphosgene (3.32 g, 11 mmol) was dissolved in a minimal amount of THF and then added to a mixture of THF (22 mL) and (S)-3-(benzyloxy)-2-hydroxypropanoic acid (2 g, 10 mmol). The mixture was stirred at room temperature overnight under an inert atmosphere. Removal of THF followed by addition of DCM (0.5 mL) and (0.5 mL) isopropyl ether yielded white crystals (0.12 g, 5% yield). ^{1}H NMR matched that of reported compound.[23]

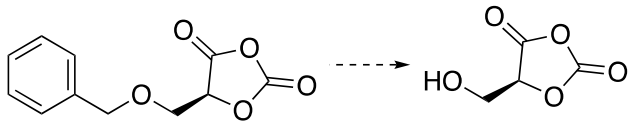

Attempted synthesis of 5-(hydroxymethyl)-1,3-dioxolane-2,4-dione (**4**): In several, separate trials, 5-((Benzyloxy)methyl)-1,3-dioxolane-2,4-dione (0.1 g 0.5 mmol) was added to various solvents (THF, toluene, acetonitrile), and the solution was flushed with nitrogen. Catalytic amounts of Pd/C (10, 20, 30%) were added to the flask. Nitrogen was removed via vacuum and replaced with hydrogen gas via a balloon. Analysis of the reaction mixture by TLC (staining with I_2 or PMA) showed only baseline spots. Crude analysis by ^{1}H NMR showed no remaining starting material; however, no product peaks could be identified.

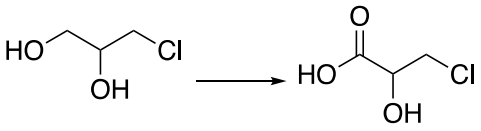

Synthesis of 3-chloro-2-hydroxypropanoic acid (**7**): 3-Chloropropane-1,2-diol (125 g, 1.13 mol) was dissolved in water (125 g) and placed in a graduated cylinder equipped with a dropping funnel the lower end of which was on the bottom of the graduated cylinder. Over a period of 2 days, HNO_3 (175 g, 2.77 mol) was dropped into the bottom of the cylinder to form a biphasic reaction mixture. Over the course of 14 days, the solution turned from clear to green, then back to clear. Once evolution of the gas ceased, the residual water was removed via distillation. Care was taken to keep the temperature of the material in the distillation flask under 80 °C. The resulting residue became crystalline upon cooling to room temperature. The crystalline material (~100 g) was then dissolved in water and, $CaCO_3$ was added until foaming

stopped.[25] The white slurry was centrifuged, and the supernatant was extracted with ether then dried over $MgSO_4$ and filtered. The resulting solution was concentrated to a yellow oil. The yellow oil was sublimed at 300 mtorr at 60 °C to yield white crystals (30 g 21% yield). ^{1}H NMR: δ 4.60 (t, 1H, *J* = 3.4 Hz), 3.90 (dd, 2H, *J* = 3.4, 1.83 Hz) ^{13}C NMR: δ 174.5, 70.4, 46.2.

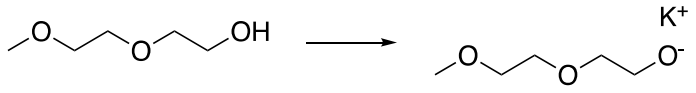

Preparation of ~0.5 M potassium 2-(2-methoxyethoxy)ethan-1-olate (K-DEG): A dry 2-neck flask with a dropping funnel was charged with THF (200 mL) under nitrogen atmosphere. Freshly cut and washed (with hexanes) potassium metal (4.7 g, 119 mmol) was added to the THF and allowed to stir for 20 minutes at room temperature. Dry 2-(2-methoxyethoxy)ethan-1-ol (DEG) (14 mL, 118 mmol) was added dropwise over 30 minutes. Once complete, the dropping funnel was replaced with a reflux condenser, and the reaction was heated to reflux for 16 hours. The solution was filtered without exposure to air and stored under nitrogen atmosphere in the refrigerator. Before each use the solution was titrated in triplicate using phenolphthalein in water and 1 M HCl to determine the concentration of alkoxide.[31]

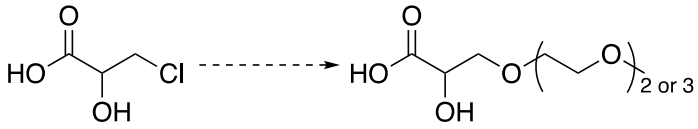

First attempted synthesis of 13-hydroxy-2,5,8,11-tetraoxatetradecan-14-oic acid (**8**): 3-Chloro-2-hydroxypropanoic acid (0.2 g, 1.6 mmol) was added to THF (10 mL) and cooled in an ice bath. Cs_2CO_3 (0.5 g, 1.6 mmol) was added to the stirred solution. A faint yellow color

was observed. In a separate flask, 60% NaH (0.06 g, 1.6 mmol) in oil was added to THF (5 mL) and cooled in an ice bath. 2-(2-methoxyethoxy)ethan-1-ol (TEG) (0.18 mL, 1.6 mmol) was added to the chilled mixture and allowed to stir. Once the evolution of gas ceased, the TEG mixture was transferred to the chloro-2-hydroxypropanoic acid mixture via cannula and allowed to warm to room temperature. After 2 hours, the crude mixture was filtered, concentrated, and a small aliquot was removed for ^{1}H NMR analysis (D_2O); only starting materials were observed. In separate experiments, the temperature was varied (room temperature and reflux), but neither of the conditions produced the desired product.

Second attempted synthesis of 13-hydroxy-2,5,8,11-tetraoxatetradecan-14-oic acid (**8**): 3-Chloro-2-hydroxypropanoic acid (0.1 g, 0.8 mmol) was added to THF (10 mL) and cooled in an ice bath. A solution of K-DEG (0.62 M, 2.5 mL, 1.6 mmol) was added and allowed to warm to room temp. After 2 hours, only starting material was observed by ^{1}H NMR. In separate experiments, heating the solution to reflux did not yield better results.

Third attempted synthesis of 13-hydroxy-2,5,8,11-tetraoxatetradecan-14-oic acid (**8**): 3-Chloro-2-hydroxypropanoic acid (0.25 g, 2 mmol) and dry acetone (20 mL) were added to a dry round-bottom flask under nitrogen atmosphere. After addition of NaI (3 g, 2 mmol), the solution turned yellow. After heating to reflux for 30 minutes, K-DEG (0.3 M, 12 mL, 4 mmol) was added and the reaction was allowed to stir overnight. The solvent was removed by rotary evaporation to yield a sticky brown solid. The solid was washed with ether (3 x 15 mL), and the filtrate was dried with $MgSO_4$ and concentrated. TLC (*p*-anisaldehyde stain) of the product

showed 2 spots (2:3 hexane: ethyl acetate). ^{1}H NMR and ^{13}C NMR led us to characterize this product as a mixture that contained 1-(2-(2-methoxyethoxy)ethoxy)propan-2-one, shown below, and DEG.

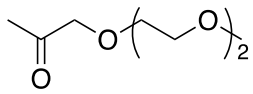

^{1}H NMR: δ 3.7 (m, 8H), 3.63 (m, 8H), 3.38 (s, 5H), 2.75 (s, 3H), 2.24 (s, 2H) ^{13}C NMR: δ 210.3, 72.2, 71.7, 69.9, 69.4, 61.3, 58.9, 31.6

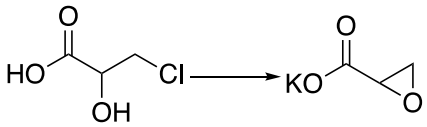

Synthesis of oxirane-2-carboxylic acid (**10**): A nearly saturated solution of KOH and methanol was shaken with silica gel for 10 minutes, filtered, and titrated to determine molarity. A solution of KOH (4.8 M, 6.7 mL, 32 mmol) was added to 3-chloro-2-hydroxypropanoic acid (2 g, 16 mmol) and dissolved in absolute methanol (10 mL) in an ice bath. The mixture was allowed to warm to room temperature and stir for 1 hour before being placed in the refrigerator overnight. The reaction was filtered, washed with MeOH, triturated into ether and filtered again to yield a white solid (0.59 g, 32% yield). ^{1}H NMR: δ 3.36 (dd, 1H, J = 2.1 Hz, 3.6 Hz), 2.94 (t, 1H, J = 4.2 Hz), 2.78 (dd, 1H, J = 4.2 Hz, 2.1 Hz).

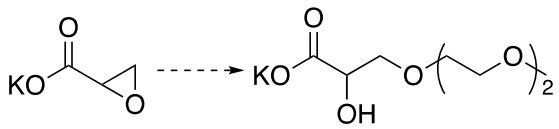

First attempted synthesis of potassium 13-hydroxy-2,5,8,11-tetraoxatetradecan-14-oate (**11**): Potassium oxirane-2-carboxylate (0.02 g, 0.15 mmol) was added to a dry vial with 18-crown-6 (0.001 g). The vial was charged with THF (3 mL) and K-DEG (0.4 M 0.19 mL, 0.08 mmol) then heated to reflux. After 2 hours, only starting material was observed by ^{1}H NMR.

Second attempted synthesis of potassium 13-hydroxy-2,5,8,11tetraoxatetradecan-14-oate (**11**): To a dry round-bottom flask, potassium oxirane-2-carboxylate (0.02 g, 0.15 mmol), DCM (3 mL), and tris(pentafluorophenyl)borane (0.004 g, 5 mol%) were added. The mixture was allowed to stir for 10 minutes under nitrogen before neat TEG (0.019 mL, 0.15 mmol) was added. The mixture was allowed to stir at room temperature overnight. Only starting material was observable by ^{1}H NMR. Attempts at heating the reaction and use of different solvents (toluene, hexane, nitromethane, chloroform) yielded similar results.

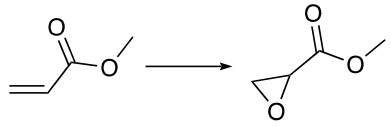

Synthesis of methyl oxirane-2-carboxylate (**13**): To a round-bottom flask, 6% NaOCl (86 mL, 0.069 mol) was added, and the flask was cooled in an ice bath. Methyl acrylate (6 g, 0.069 mol) was then added. The mixture was stirred for 30 minutes. The ice bath was then removed, and the reaction was allowed to stir for 1.5 hours. The mixture was extracted with DCM (3 x

50 mL), and the combined organic layers were dried using $MgSO_4$, filtered, and concentrated *in vacuo* to produce a yellow oil. Distillation of the oil (50 mmHg, 45-47 °C) yielded pure product in 30% yield. ^{1}H NMR matched that of the reported compound.[27]

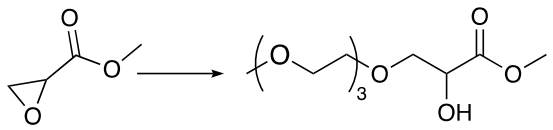

Synthesis of methyl 13-hydroxy-2,5,8,11-tetraoxatetradecan-14-oate (**15**): TEG (0.08 g, 0.7 mmol) was added to a vial with a $Mg(ClO_4)_2$ (0.02 g, 0.09 mmol) and allowed to stir briefly before methyl oxirane-2-carboxylate (0.036 g, 0.35 mmol) was added to the vial. The vial was tightly capped and heated to 65 °C for 2 days. The vial was cooled to room temperature, and water (5 mL) was added to the mixture. The aqueous layer was extracted with ether (4 x 5 mL), and the combined organic fractions were dried over $MgSO_4$, filtered, and concentrated *in vacuo* to yield a yellow oil (50%). ^{1}H NMR: δ 4.33 (m, 1H), 3.79 (m, 2H), 3.65 (S, 3H), 3.70 (m, 2H), 3.65 (m, 2H), 3.56 (m, 2H), 3.38 (s, 3H).

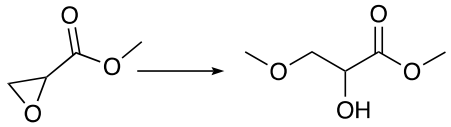

Synthesis of 2-hydroxy-3-methoxypropanoic acid (**14**): Methyl 2-hydroxy-3-methoxypropanoate (0.5 g, 9 mmol) was added to a vial and chilled in an ice bath. Next, KOH in methanol (2 M, 5.5 mL, 11 mmol) was added. The yellow reaction mixture was removed from the ice bath and allowed to stir at room temperature until complete by TLC analysis (ceric

ammonium molybdate stain, 60:40 ethyl acetate: hexanes). The reaction was concentrated and acidified with cold HCl (6 M). The filtrate was collected after removal of the white solid via vacuum filtration. The clear liquid was then triturated into acetone and filtered. The slurry was dried using $MgSO_4$, filtered and concentrated; this cycle was repeated 3 times to yield a brown oil (0.73 g, 82%) ^{1}H NMR: δ 4.27 (dd, 1H, J = 3.0 Hz, 3.9 Hz) 3.63 (m, 2H) 3.32 (s, 3H)

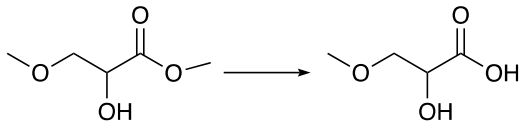

Synthesis of 2-hydroxy-3-methoxypropanoic acid (**16**): Methyl 2-hydroxy-3-methoxypropanoate (0.5 g, 9 mmol) was added to a vial and chilled in an ice bath. Next, KOH in methanol (2 M, 5.5 mL, 11 mmol) was added. The yellow reaction mixture was removed from the ice bath and allowed to stir at room temperature until complete by TLC analysis (ceric ammonium molybdate stain, 60:40 ethyl acetate: hexanes). The reaction was concentrated and acidified with cold HCl (6 M). The filtrate was collected after removal of the white solid via vacuum filtration. The clear liquid was then triturated into acetone and filtered. The slurry was dried using $MgSO_4$, filtered and concentrated; this cycle was repeated 3 times to yield a brown oil (0.76 g, 70%) ^{1}H NMR: δ 4.27 (dd, 1H, J = 3.0 Hz, 3.9 Hz) 3.63 (m, 2H) 3.32 (s, 3H)

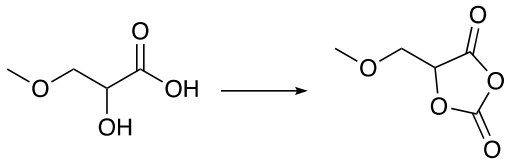

Attempted Synthesis of 5-(methoxymethyl)-1,3-dioxolane-2,4-dione (**18**): Triphosgene was dissolved in dry dioxane. The mixture was then transferred via cannula to a flask containing 2-hydroxy-3-methoxypropanoic acid which had residual water removed via addition and removal of toluene *in vacuo*. The mixture was allowed to stir at room temperature overnight. Solvents were then removed, and the flask was moved into a glovebox. Column chromatography using dry silica (150 °C, 48 hours, 300 mTorr) eluting with varying dry solvent mixtures (hexanes, ethyl acetate, THF) was unsuccessful in purifying the product.

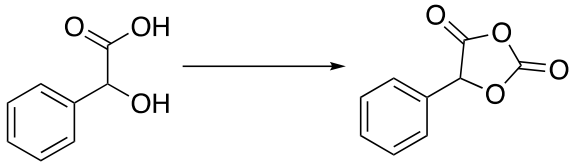

Synthesis of 5-phenyl-1,3-dioxolane-2,4-dione (**21**): In a Schlenk flask, mandelic acid (6.0 g, 39 mmol) and activated carbon (580 mg) were dissolved in dry THF (70 mL). Diphosgene (5.5 mL, 46 mmol) was added to the flask via syringe under nitrogen. The reaction stirred at room temperature overnight. The next day the mixture was filtered through celite then washed with THF. The THF was removed to yield a viscous yellow oil. The oil was quickly transferred to a vial and was layered with hexanes (~10 mL). Storage in the freezer overnight yielded white crystals which were isolated quickly via vacuum filtration. The crystals were washed with hexanes then dried *in vacuo*. Yield 2.7 g 38 % ^{1}H NMR matched that of previously reported.[30]

Preparation of Poly(mandelic acid) brushes

The synthesis of mandelic acid-derived polymer brushes was carried out using surface initiated ring opening polymerization (SIP) from silicon substrates. Silicon wafers (wafer world) were cut into ~3 cm squares washed with hexanes, water, and ethanol. Wafers were then sonicated in ethanol for 2 min, dried with a nitrogen stream, and exposed to UV-Ozone irradiation for 30 min. After exposure, the wafers were placed into vials and transferred into a glovebox. Solutions of mandelic acid OCA (2.5 mL of 0.62 M) and pyridine (0.23 mL of 0.13M) were added to the wafers. The vials were sealed with Teflon tape and electrical tape, removed from the glove box, and placed on as shaker table at 200 RPM. After a given time the wafers were removed and washed with water and ethanol. Wafers were then sonicated in chloroform to remove any unreacted monomer. Thicknesses were characterized using variable angle spectroscopic ellipsometry (VASE). The thickness of the polymer brush was modeled using a Cauchy layer on Silicon substrate.

References

(1) Albertsson, A. C.; Varma, I. K. Recent Developments in Ring Opening Polymerization of Lactones for Biomedical Applications. *Biomacromolecules* **2003**, *4* (6), 1466–1486.

(2) Bhat, S.; Kumar, A. Biomaterials and Bioengineering Tomorrow's Healthcare. *Biomatter*. Taylor & Francis 2013.

(3) Migonney, V. History of Biomaterials. In *Biomaterials*; John Wiley & Sons, Inc.: Hoboken, NJ, USA, 2014; pp 1–10.

(4) Kamber, N. E.; Jeong, W.; Waymouth, R. M.; Pratt, R. C.; Lohmeijer, B. G. G.; Hedrick, J. L. Organocatalytic Ring-Opening Polymerization. *Chem. Rev.* **2007**, *107* (12), 5813–5840.

(5) Kowalski, A.; Duda, A.; Penczek, S. Kinetics and Mechanism of Cyclic Esters Polymerization Initiated with Tin(II) Octoate. 3. Polymerization of L , L -Dilactide. *Macromolecules* **2000**, *33* (20), 7359–7370.

(6) Lahann, J.; Langer, R. Surface-Initiated Ring-Opening Polymerization of ε-Caprolactone from a Patterned Poly(Hydroxymethyl-p-Xylylene). *Macromol. Rapid Commun.* **2001**, *22* (12), 968–971.

(7) Möller, M.; Nederberg, F.; Lim, L. S.; Kånge, R.; Hawker, C. J.; Hedrick, J. L.; Gu, Y.; Shah, R.; Abbott, N. L. Stannous(II) Trifluoromethane Sulfonate: A Versatile Catalyst for the Controlled Ring-Opening Polymerization of Lactides: Formation of Stereoregular Surfaces from Polylactide "Brushes." *J. Polym. Sci. Part A Polym. Chem.* **2001**, *39* (20), 3529–3538.

(8) Choi, I. S.; Langer, R. Surface-Initiated Polymerization of L-Lactide: Coating of Solid

Substrates with a Biodegradable Polymer. *Macromolecules* **2001**, *34* (16), 5361–5363.

(9) Pounder, R. J.; Dove, A. P. Towards Poly(Ester) Nanoparticles: Recent Advances in the Synthesis of Functional Poly(Ester)s by Ring-Opening Polymerization. *Polym. Chem.* **2010**, *1* (3), 260–271.

(10) Williams, C. K. Synthesis of Functionalized Biodegradable Polyesters. *Chem. Soc. Rev.* **2007**, *36* (10), 1573.

(11) Thillaye du Boullay, O.; Marchal, E.; Martin-Vaca, B.; Cossío, F. P.; Bourissou, D. An Activated Equivalent of Lactide toward Organocatalytic Ring-Opening Polymerization. *J. Am. Chem. Soc.* **2006**, *128* (51), 16442–16443.

(12) Martin Vaca, B.; Bourissou, D. O -Carboxyanhydrides: Useful Tools for the Preparation of Well-Defined Functionalized Polyesters. *ACS Macro Lett.* **2015**, 792–798.

(13) Rubinshtein, M.; James, C. R.; Young, J. L.; Ma, Y. J.; Kobayashi, Y.; Gianneschi, N. C.; Yang, J. Facile Procedure for Generating Side Chain Functionalized Poly(α-Hydroxy Acid) Copolymers from Aldehydes via a Versatile Passerini-Type Condensation. *Org. Lett.* **2010**, *12* (15), 3560–3563.

(14) Jiang, X.; Vogel, E. B.; Smith, M. R.; Baker, G. L. Amphiphilic PEG/Alkyl-Grafted Comb Polylactides. *J. Polym. Sci. Part A Polym. Chem.* **2007**, *45* (22), 5227–5236.

(15) Rieger, J.; Bernaerts, K. V.; Du Prez, F. E.; Jérôme, R.; Jérôme, C. Lactone End-Capped Poly(Ethylene Oxide) as a New Building Block for Biomaterials. *Macromolecules* **2004**, *37* (26), 9738–9745.

(16) Davies, W. H. Anhydrocarboxy-Derivatives of Hydroxy- and Mercapto-Acids. *J. Chem. Soc.* **1951**, 1357.

(17) Thillaye du Boullay, O.; Bonduelle, C.; Martin-Vaca, B.; Bourissou, D. Functionalized Polyesters from Organocatalyzed ROP of GluOCA, the O-Carboxyanhydride Derived from Glutamic Acid. *Chem. Commun.* **2008**, No. 15, 1786–1788.

(18) Kricheldorf, H.; Jont, J. M. New Polymer Syntheses 8. Synthesis and Polymerization of L-Lactic Acid O-Carboxyanhydride (5-MethyI-Dioxolan-2,4-Dione). *Polym. Bull.* **1983**, *9* (6–7), 276–283.

(19) Cavelier, F. First Synthesis of the Enantiomerically Pure α-Hydroxy Analogue of S-Tert- Butyl Cysteine Florine. *Tetrahedron: Asymmetry* **1997**, *8* (1), 41–43.

(20) Leemhuis, M.; van Nostrum, C. F.; Kruijtzer, J. A. W.; Zhong, Z. Y.; ten Breteler, M. R.; Dijkstra, P. J.; Feijen, J.; Hennink, W. E. Functionalized Poly(α-Hydroxy Acid)s via Ring-Opening Polymerization: Toward Hydrophilic Polyesters with Pendant Hydroxyl Groups. *Macromolecules* **2006**, *39* (10), 3500–3508.

(21) Chen, X.; Lai, H.; Xiao, C.; Tian, H.; Chen, X.; Tao, Y.; Wang, X. New Bio-Renewable Polyester with Rich Side Amino Groups from L-Lysine via Controlled Ring-Opening Polymerization. *Polym. Chem.* **2014**, *5* (22), 6495–6502.

(22) *Poly(Ethylene Glycol) Chemistry*; Harris, J. M., Ed.; Springer US: Boston, MA, 1992.

(23) Lu, Y.; Yin, L.; Zhang, Y.; Zhonghai, Z.; Xu, Y.; Tong, R.; Cheng, J. Synthesis of Water-Soluble Poly(α-Hydroxy Acids) from Living Ring-Opening Polymerization of O-Benzyl-L-Serine Carboxyanhydrides. *ACS Macro Lett.* **2012**, *1* (4), 441–444.

(24) Kramer, J. R.; Deming, T. J. General Method for Purification of α-Amino Acid-n-Carboxyanhydrides Using Flash Chromatography. *Biomacromolecules* **2010**, *11* (12), 3668–3672.

(25) Koelsch, C. F. A Sulfer Analog of Glyceric Acid. Beta-Thioglyceric Acid. *J. Am. Chem. Soc.* **1930**, *52* (3), 1105–1108.

(26) Blau, N. F.; Johnson, J. W.; Stuckwisch, C. G. The Synthesis of Dimethyl-(α-Hydroxy-β-Propiothetin) Hydrochloride and Related Compounds. *J. Am. Chem. Soc.* **1954**, *76* (20), 5106–5107.

(27) Stevenson, C. P.; Nielsen, L. P. C.; Jacobsen, E. N.; McKinley, J. D.; White, T. D.; Couturier, M. A.; Ragan, J. Preparation of (S)-Methyl Glycidate Via Hydrolytic Kinetic Resolution. *Org. Synth.* **2006**, *83*, 162.

(28) Hu, X.; Hu, G.; Crawford, K.; Gorman, C. B. Comparison of the Growth and Degradation of Poly(Glycolic Acid) and Poly(ε-Caprolactone) Brushes. *J. Polym. Sci. Part A Polym. Chem.* **2013**, *51* (21), 4643–4649.

(29) Hu, X.; Gorman, C. B. Resisting Protein Adsorption on Biodegradable Polyester Brushes. *Acta Biomater.* **2014**, *10* (8), 3497–3504.

(30) Buchard, A.; Carbery, D. R.; Davidson, M. G.; Ivanova, P. K.; Jeffery, B. J.; Kociok-Köhn, G. I.; Lowe, J. P. Preparation of Stereoregular Isotactic Poly(Mandelic Acid) through Organocatalytic Ring-Opening Polymerization of a Cyclic O-Carboxyanhydride. *Angew. Chemie - Int. Ed.* **2014**, *53* (50), 13858–13861.

(31) Kang, K. X.; Liu, M. Y.; Zhao, Q. X.; Fu, P.; Wang, X. B. Poly(Ethylene Oxide)-B-Poly(ε-Caprolactone) Amphiphilic Block Copolymers: Synthesis and Self-Assembly. *Adv. Mater. Res.* **2011**, *284–286*, 1877–1885.

Chapter 3

Introduction

After the failure to synthesize the OEG-OCA brushes, synthetic efforts were directed toward creation of an OEG-cyclic diester. Previously our group had demonstrated that polyester brushes could be grown from native Si-O-H groups on silicon using the cyclic diesters lactide and glycolide.[1,2] Baker et al. reported the synthesis of a number of cyclic diester derivatives including one with pendant OEG-side chains; however, that cyclic diester derivative contained a large alkyl chain between the cyclic diester and the oligo(ethylene glycol) (OEG) unit.[3–6] While the OEG functionality should impart some protein resistance there are concerns that the greasy hydrophobic alkyl spacer would negate those effects. Exploration of some cyclic diester derivatives that omit that alkyl chain is described below.

Another route explored was the polymerization of cyclic diesters from silicon that could be functionalized after polymer brush formation. This post-polymerization modification (PPM) approach has been utilized a number of times with different functionalities.[7] Development of this approach was particularly interesting because it could allow for testing of a variety of functionalities not just OEG.

Some of the most common PPM functionalities used are functional groups found in "click chemistry" reactions. Click chemistry was first defined by Sharpless as reactions that are "high yielding, wide in scope, create only byproducts that can be removed without chromatography, are stereospecific, simple to perform, and can be conducted in easily removable or benign solvents."[8] Currently there are several categories of "click" or "click like" reactions these include: 1) [3+2] cycloadditions, 2) thiol-ene,[9] 3) thiol-yne,[10] 4) select Diels-

Alder reactions and 5) nucleophilic substitution reactions on small strained rings such as epoxides.[11] The most ubiquitous "click" reaction is the copper catalyzed Huisgen 1,3-dipolar cycloaddition. [12]

Cheng and coworkers have synthesized an OCA monomer with an alkyne side chain. This side chain was functionalized at >98% with 2-aminoethanethiol utilizing thiol-yne "click chemistry" after polymerization. For their study the pendant amine group was used because PAHA containing amine functionalities have been shown to penetrate cells for gene delivery. This work demonstrates a great example of the utility of the alkyne side chain on a polymer.[13]

In another example of PPM of the alkyne functionality Shastri et al. demonstrated the use of degradable aliphatic polyesters with organic dyes. The synthesized co-polymers were modified using 1,3 dipolar additions to give polyesters with organic dyes. The co-polymers were converted into nanoparticles to test their viability as a cell imaging *in vivo*. It was shown that the dye molecules functionality (labeling of cell) was not impeded by the grafting process. Additionally, cytotoxicity studies showed good cell viability with the nanoparticles.[14]

Collard et al. showed that alkene-containing copolylactide could be modified using "thiol-ene click chemistry." Their system required the synthesis of a chlorolactide monomer that could be co-polymerized with poly (lactic acid) (PLA). A dehydrochlorination reaction using Hunig's base showed minimal degradation of the backbone and gave them access to the alkene functionality. Radical thiol-ene reactions showed a competition between functionalization and crosslinking of the alkene functionalities along the backbone. However, Michael Additions to the copolymer showed almost quantitative addition without the competing crosslinking reaction.[15]

Baker et al had previously developed an alkyne glycolide derivative for bulk polymerization.[4] They showed that in solution copper catalyzed azide-alkyne click chemistry could be used to functionalize the polyester. Their interest in appending side chain functionalities was in developing thermoresponsive polymers. Use of their monomer in conjunction with the chemistry developed for surface initiated ring-opening polymerization of cyclic diesters from silica could yield an interesting modular material for studies.

Results and discussion

Attempts to prepare a cyclic diester containing an appended OEG chain

Given the difficulty in preparing the OEG-OCA an alternative route was sought. It was envisioned that the OEG-α-hydroxy acid previously synthesized (Chapter 2 Scheme 4) could be dimerized and subsequently polymerized from the silicon surface. There are two general ways to dimerize α-hydroxy acids 1) the use of an acid catalyst (often *p*-toluenesulfonic acid) and heat to dimerize the α-hydroxy acid to the corresponding cyclic diester. 2) through the use of step-by-step condensation of the α-hydroxy acid to an α-halo-acyl halide followed by base mediated cyclization (Scheme 6).[16]

Scheme 6: General routes to cyclic diesters from α-hydroxy acids

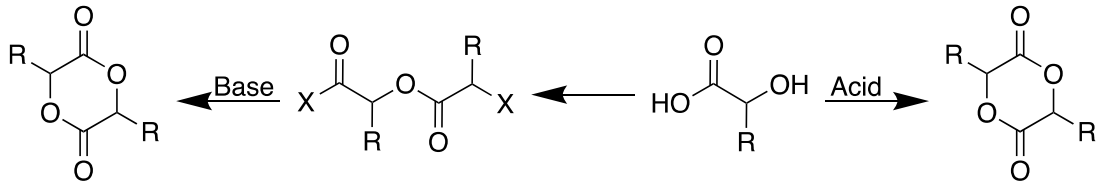

The α-hydroxy acid 2-hydroxy-3-methoxypropanoic acid (chapter 2 Scheme 4) had previously been synthesized; it was used as a model compound to develop a route to the cyclic

diester. In a first attempt the methoxy-α-hydroxy acid (**1**) was condensed with *p*-toluenesulfonic acid. After 72 hours of refluxing no starting material remained and no signals consistent with the desired product or the corresponding oligomers were observed by ^{1}H NMR.

Scheme 7: Attempted dimerization of methoxy α-hydroxy acid to the cyclic diester

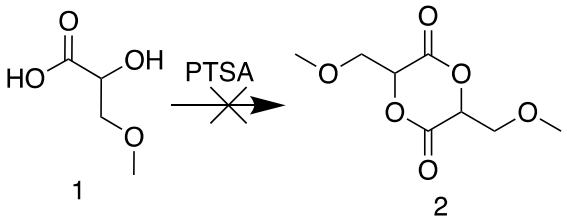

In a second attempt to synthesize the desired cyclic diester (**2**) methoxy-α-hydroxy acid (**1**) was reacted with freshly distilled $SOCl_2$ with the goal of forming either the diester directly or an α-hydroxy acid ester (Scheme 8). After stirring overnight at room temperature an aliquot was removed and tested by ^{1}H NMR. No resonances consistent with the starting material or either desired product were observed.

Scheme 8: Attempted synthesis of diester or α-hydroxy acid ester from methoxy-α-hydroxy acid using thionyl chloride

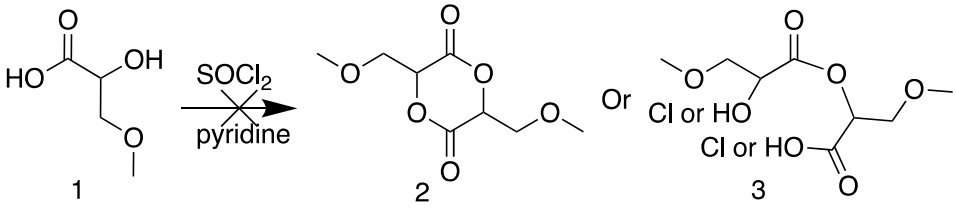

Given the difficulty in synthesizing the symmetric dimer an asymmetric dimerization was attempted. While this route would cut the side chain functionality in half but it would create an interesting system to study. To do this methoxy-α-hydroxy acid was reacted with 2-

chloroacetyl chloride in the presence of triethylamine (Scheme 9).[17] After 18 hours ^{1}H NMR showed no peaks consistent with the desired product.

Scheme 9: Attempted synthesis of an unsymmetric diester using methoxy-α-hydroxy acid and 2-chloroacetyl chloride.

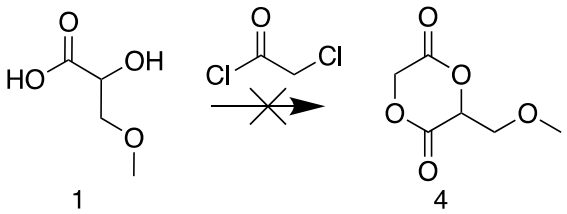

Given the synthetic difficulty in developing new monomers with ether containing side chains a new route was needed. Preparation of a cyclic diester hinges upon driving the equilibrium between cyclization and polymerization by removal of the cyclic diester from the reaction as it is formed. In retrospect, Baker had to distill his monomers at very high temperatures/low pressures with increasingly low yields.[5] Indeed, Weck resorted to the hemi-lactide and activated it by Finklestein reaction.[18] Gurny reported several alkyl and benzyl derivatives that were almost all produced in low yields <50%.[19] Further synthetic efforts were directed toward a post-polymerization modification strategy.

Synthesis of a "clickable" monomer

Propargyl glycolide (**8**) was initially synthesized follow the reported procedure outlined by Baker.[4] Propargyl bromide (**5**) and ethyl glyoxylate were coupled under Barbier conditions to give ethyl 2-hydroxypent-4-ynoate in moderate yields (55%) after column chromatography and distillation. Hydrolysis of the ester (**6**) to produce the α-hydroxy acid (**7**) was accomplished in moderate yields (40%). Dimerization of the α-hydroxy acid (**7**) to give the alkyne-appended

lactide (PPGL) (**8**) in the presence of *p*-toluenesulfonic acid (PTSA) was accomplished in low (23%) yields (**Scheme 10**).

Scheme 10: Synthesis of propargyl glycolide monomer (PPGL)

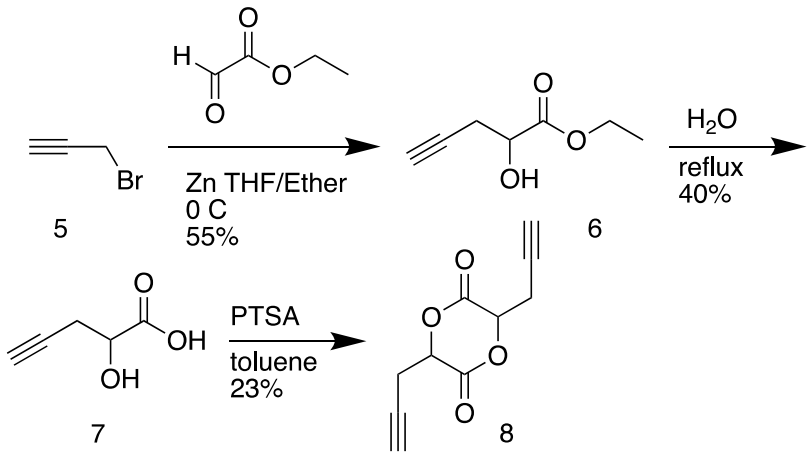

Given the low yield in the saponification step, another approach to the α-hydroxy acid was sought. A literature review led to a report where the α-hydroxy acid could be synthesized from diethyl 2-acetamidomalonate.[20] While this procedure was not as atom economical as the previous one; however, it did have the advantages of no chromatography and no distillation. Diethyl 2-acetamidomalonate (**9**) was alkylated under basic conditions using potassium tert-butoxide and freshly prepared propargyl tosylate to give the propargyl derivative (**10**). Refluxing of compound **10** in 2 M sulfuric acid resulting in the intermediate α-amino acid (**11**) which was treated with sodium nitrate without further purification to yield the desired α-hydroxy acid in 35% yield. While the yield for this step is lower than previously outlined procedure the overall yield to the α-hydroxy acid is greater. Additionally, this route has been scaled to make gram quantities of the α-hydroxy acid and does not require distillation or chromatography. In conclusion, the combination of the two approaches above yielded gram

quantities of an alkyne monomer that would be used for further investigations of polymer brush growth and PPM.

Scheme 11: Alternative synthesis of propargyl α-hydroxy acid

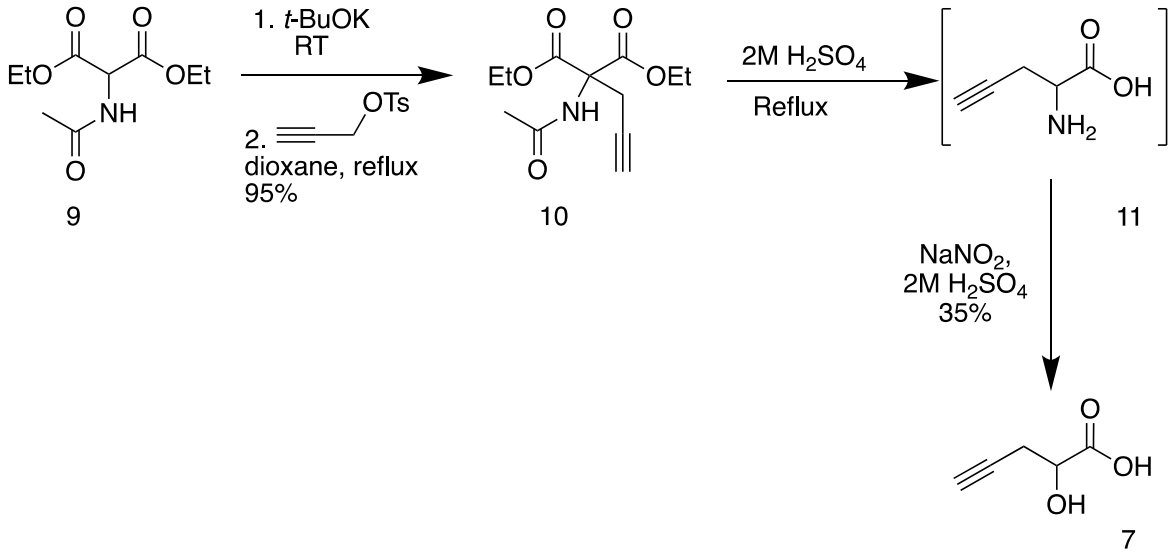

Growth of PPGL Brushes

To examine the surface initiated ring-opening polymerization of PPGL from silicon oxide a variety of conditions were examined. Initially the conditions reported by Xu and Hu to grow poly(lactic acid) brushes were used (0.1 M monomer, 0.001 M $Sn(Oct)_2$, in tetrahydrofuran (THF) for 24 hours at 25 °C).[1,21] When those conditions were used with the PPGL monomer they showed minimal (2.7 nm) growth. A study was undertaken to examine a variety of growth conditions for this new monomer system.

Table 2: PPGL polymer brush growth conditions in THF varying concentration and temperature for 24 hours

Monomer Concentration (M)	Temperature (°C)	Ellipsometric Thickness nm (stdev)
0.1	25	2.7 (1.6)
0.1	40	4.3 (1.5)
0.5	40	6.7 (1.1)
0.5	60	9.6 (2.4)

Initially, the effect of temperature at fixed concentration and time was examined. When the temperature was raised to 40 °C no additional growth was observed. Next, the effect of higher monomer concentration was examined. The use of a higher concentration of monomer in solution gave brushes of longer length (6.7 compared to 4.3 nm) when the temperature was increased to 60 °C brushes of 9.6 nm could be achieved.

In another experiment the growth of PPGL brushes were examined using acetonitrile. It was initially hypothesized that a more polar solvent than THF may give longer brushes. The use of a new catalyst(1,5,7-triazabicyclo[4.4.0]dec-5-ene or TBD) was also examined. Polymer brushes of 11.2 nm could be achieved utilizing the $Sn(Oct)_2$ catalyst after 24 hours, however; additional reaction time showed that the polymer brushes decreased in thickness.

When TBD was utilized as a catalyst the maximum achievable height was 10.2 nm at 36 hours. Again, at longer reaction times the thickness of the polymer brushes decreased significantly. A thickness of only 6.0 nm was obtained after 48 hours.

This phenomenon of longer reaction times reducing the height of polymer brushes could be attributed to: 1.) chain transfer events in which the polymer brush chains are

transferred to polymer chains growing in solution–the steric repulsions of the polymer brush may not allow for chain transfer back to active chains on the surface. 2.) Chain scission events in which the active chain reacts with itself or another polymer brush chain to cleave the chain thus decreasing the thickness of the brush. 3) Back-biting of the chain end to generate the monomer (equilibrium between monomer and polymer).[22]

Table 3: PPGL polymer brush growth conditions in acetonitrile (0.2 M) at 25 °C varying catalyst and time

Catalyst	Time (h)	Ellipsometric thickness (nm) (stdev)
$Sn(Oct)_2$	12	7.8 (1.4)
$Sn(Oct)_2$	24	11.2 (0.9)
$Sn(Oct)_2$	36	8.60 (0.8)
$Sn(Oct)_2$	48	8.7 (1.7)
TBD	12	7.7 (0.9)
TBD	24	8.2 (1.2)
TBD	36	10.2 (0.2)
TBD	48	6.0 (0.3)

The effects of solvent and time were examined to determine the maximum thickness of PPGL brushes. PPGL brushes were grown at 0.1 M concentration of monomer and 0.001 M $Sn(Oct)_2$ at 40 °C for 12 and 24 hours in different solvents. In acetonitrile brushes of 19.4 nm could be achieved after 24 hours. The use of THF gave brushes that were much shorter, only 4.3 nm after 24 hours. When toluene was used brushes of up to 41.7 nm could be achieved. This dramatic increase in thickness could be attributed to the lower solubility of the monomer

in toluene. This lower solubility could create a driving force for monomer and propagating chain end interactions.

Table 4: PPGL polymer brush growth conditions in different solvents and times at 40 C, 0.1 M, Sn(Oct)2

Solvent	Time	Ellipsometric thickness nm (stdev)
acetonitrile	12	7.62 (1.4)
acetonitrile	24	19.4 (0.4)
THF	12	2.5 (0.3)
THF	24	4.3 (1.5)
toluene	12	15.2 (1.3)
toluene	24	41.7 (2.3)

To investigate the reproducibility of brush growth three sets of five silicon wafers were used to grow poly(propargylglycolide) brushes from surface silanol groups. Each set had a wafer removed every six hours for measurements. Figure 11 shows that with increased reaction time the thickness of the polymer brushes increased. At shorter (<18 hours) reaction times the measurements are in good agreement between sets; at longer reaction times (24 hours) the thickness of the films varied significantly from 23 to 41 nm. It is hypothesized that the poly dispersity within the polymer brushes is a result of chain termination events that occur because of trace impurities in solution. This linear trend is initially in good agreement with the previously reported growth of PLA. However, when PLA was grown the system began to plateau around 10 nm of growth compared to this system which continues to trend in a linear manor. This discrepancy in growth kinetics could be attributed to the grafting density of the

system. PLA may have a higher grafting density thus creating less polydispersity and allowing propagating chain ends to get buried in the polymer brush matrix compared to this PPGL system which may have a higher polydispersity thus allowing chain ends to continue propagating. There may also be solvent effects that contribute to growth kinetics.

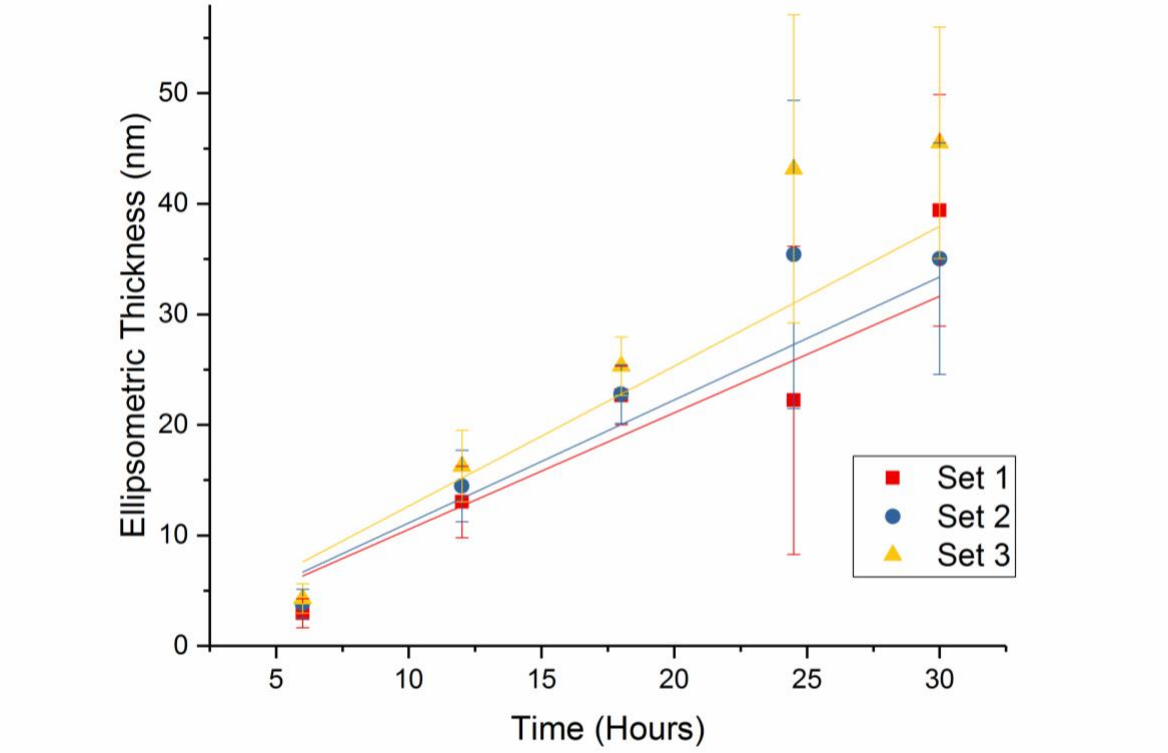

Figure 11: Plots of ellipsometric thicknesses of PPGL brushes from surface silanol groups versus growth time. Reaction conditions: [meso/rac-3,6-di-2-propynyl-1,4-dioxane-2,5-dione] 0.1 M, [Sn(Oct)2] 0.007 M in toluene, 40 ºC. Error bars represent magnitude of 90% confidence interval for 3 measurements on a single wafer. Lines are draw as a guide for the eye.

Functionalizing PPGL with OEG

After the fabrication of PPGL brushes, experiments were undertaken to appended OEG side chains to the polymer brushes. Previously, poly(ethylene glycol) (PEG) had been appended to the bulk polymer to create bottle brush polymers.[4] With no accurate way to determine the

amount of polymer brush on the surface molar ratios for appending OEG were made assuming all of the monomer in solution was polymerized from the surface. A large excess (>12x) of OEG-azide[23,24] was dissolved in DMF with ascorbic acid and added to the PPGL polymer brushes in the glovebox. After addition of $CuSO_4$ to the vials they were capped, removed, and allowed to stir at room temperature for 24 hours. After washing the OEG-PPGL brushes with water and ethanol they were used for further characterization and studies.

The thickness of the PPGL polymer brushes were measured before and after grafting OEG to the polymer chains. Figure 12 shows four different PPGL polymer brushes of varying thicknesses and the resulting ellipsometric thickness after grafting OEG to them. For all polymer brushes, there is an increase of 10-26% in the thickness of the film after functionalization with OEG. This increase in thickness is attributed elongation of the height of the brushes due to the steric repulsions of the grafted side chains (Figure 13) and is consistent with previous reports.[25]

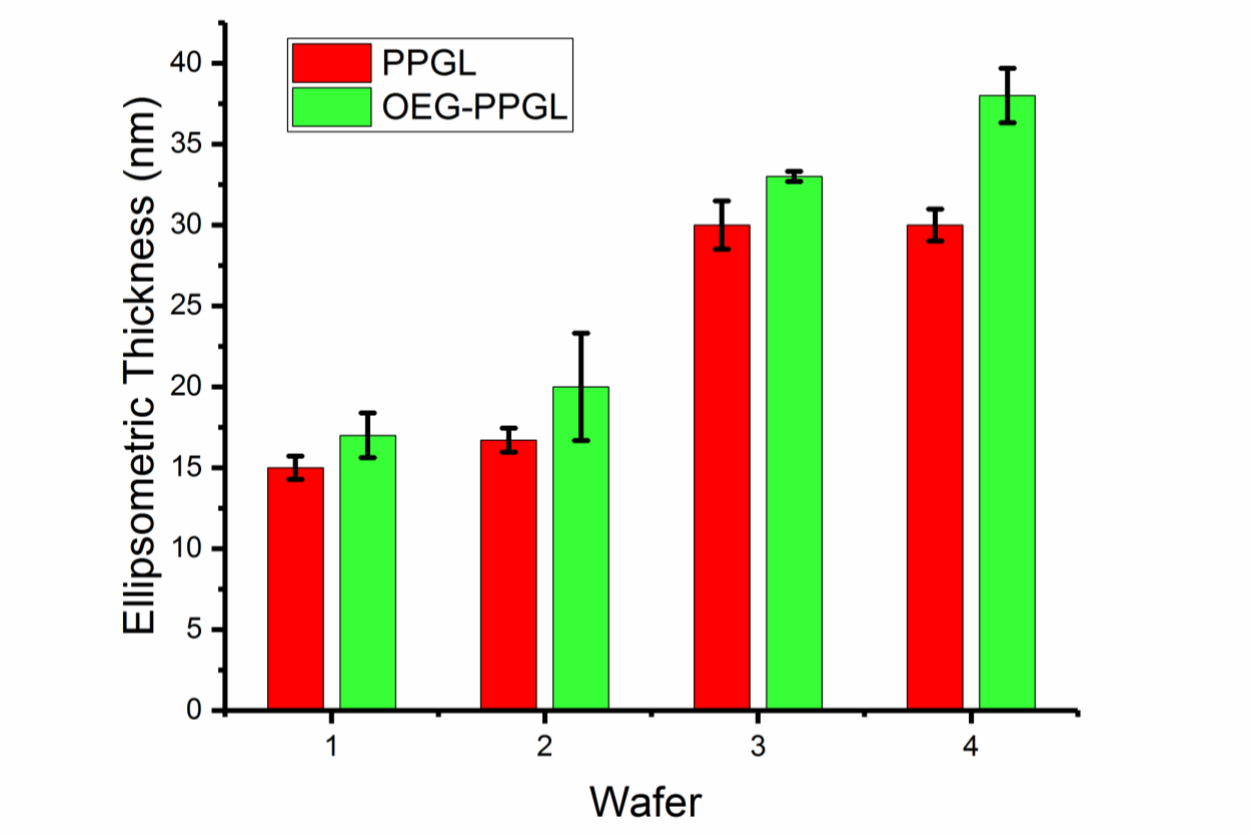

Figure 12: Bar graph of different polymer brush wafers before (red) and after (green) grafting OEG

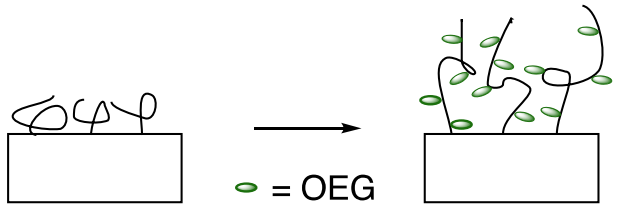

Figure 13: Cartoon representation of PPGL elongating because of the OEG functionalization

Water contact angle measurements of PPGL and OEG-PPGL polymer brushes

To measure the relative hydrophilicity of the polymer brushes, water contact angle measurements were made before and after grafting OEG side chains to the PPGL brushes (Figure 14). Water contact angle measurements on the native PPGL brushes were ca. 75º. This

number is in good agreement with that reported previously for PLA brushes which showed a static water contact angle measurement of 80º. After functionalizing the brushes with OEG the water contact angle was ca. 38º. This large increase in hydrophilicity can be attributed to the incorporation of the OEG side chains into the brush. Native PEG has a reported water contact angle of ~22º.[26]

Figure 14: Typical advancing water contact angle measurements of PPGL brushes (left) and OEG- PPGL brushes (right).

ATR-FTIR measurements of PPGL and OEG-PPGL polymer brushes

ATR-FTIR spectra where taken of the polymer brush before and after functionalization. The C=O stretch correlating to the polyester along the backbone of the polymer brush can be observed at ~1750 cm^{-1} for both the PPGL and PPGL-OEG brush. Stretches for the terminal alkyne C-H of the PPGL brush can be observed at ~3282 cm^{-1} This stretch disappears when exposed to the "click" reaction conditions indicative of loss of the alkyne species.

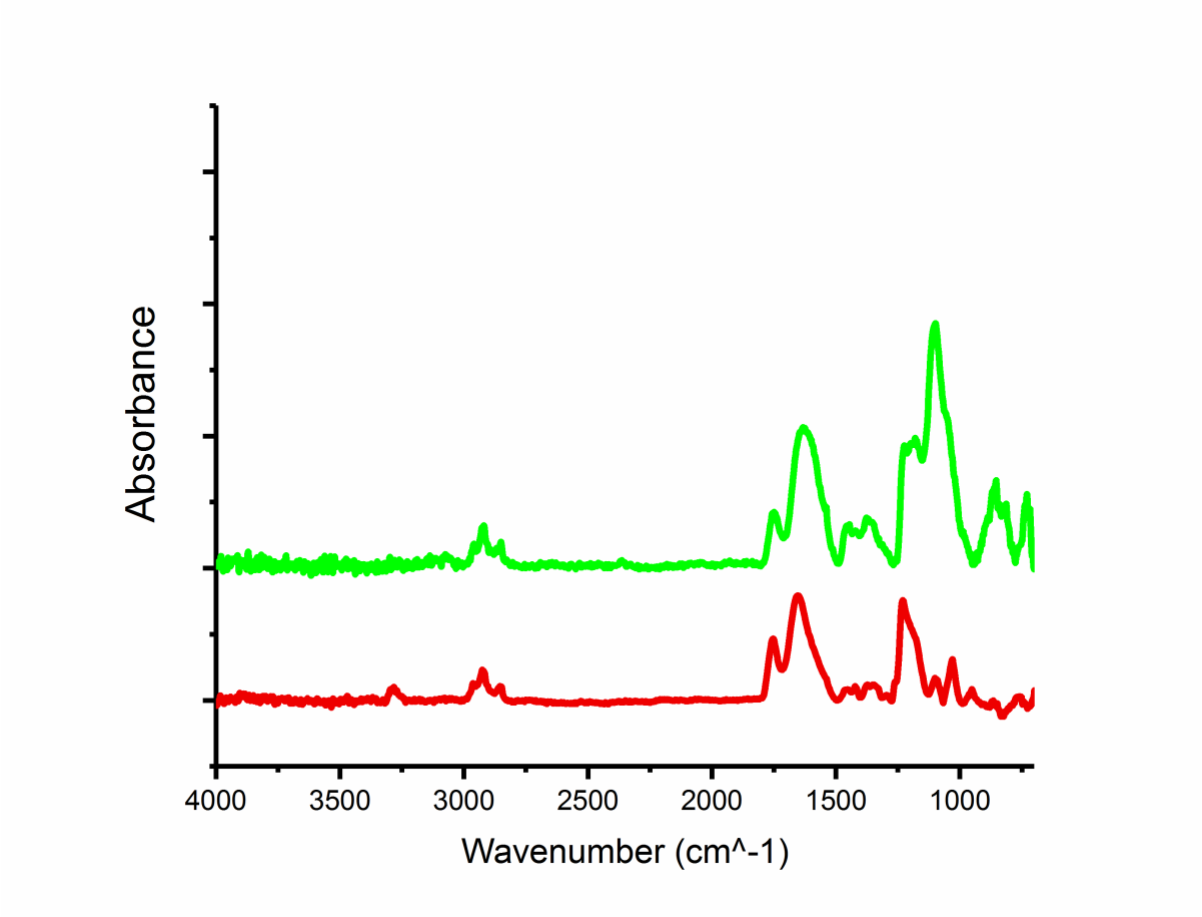

Figure 15: Typical ATR–FTIR spectrum of polymer brushes grown on Si/SiOx Top (green): PPGL brushes after exposure to click reaction conditions. Reaction conditions: [DEG-N3] 0.77 mmol, [Sodium ascorbate] 0.031 mmol, [CuSO4] 0.039 mmol. Bottom (red): native PPGL brushes

Experimental

Ellipsometric Thickness Measurements: Ellipsometric thickness was measured using a variable angle spectroscopic ellipsometry (VASE, J.A. Woollam) at a 55, 65, and 75 angle of incidence to determine the thickness of polymer layers. Polymer brush layers were modeled as a Cauchy layer.

ATR-FTIR: Data were collected on a Thermo scientific Nicolet 6700 Attenuated Total Reflectance Fourier Transform Infrared spectrometer using a germanium crystal. Background spectra were collected and corrected in air. 512 scans were taken of wafers that were placed in contact with the crystal with pressure applied via the hammer.

Water contact angle: A goniometer (OCA-10, Data Physics) measured the advancing and receding water contact angles using 3 μL droplets of water as probe liquid. The average of 3–5 measurements is reported.

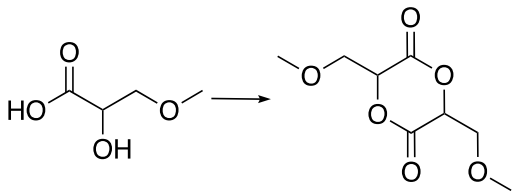

Attempted synthesis of 3,6-bis(methoxymethyl)-1,4-dioxane-2,5-dione (**1**): 2-hydroxy-3-methoxypropanoic acid (0.1 g, 0.8 mmol) and *p*-toluene sulfonic acid (14 mg, 0.08 mmol) were added to a flask charged with toluene (50 mL) and equipped with a Dean-Stark trap. The mixture was refluxed for 24 hours. Crude ^{1}H NMR showed peaks that could not be assigned to the desired product.

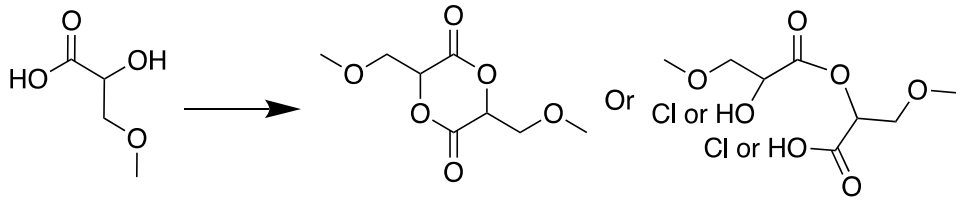

Attempted dimerization of 2-hydroxy-3-methoxypropanoic acid with thionyl chloride (**3**): 2-hydroxy-3-methoxypropanoic acid (0.12 g, 0.1 mmol) was dissolved in pyridine (5 mL, 0.62 mmol) in a nitrogen purged dry round bottom flask. Thionyl chloride (4.5 mL, 0.62 mmol) was added dropwise at room temperature over 30 minutes. The mixture was allowed to stir overnight. Crude ^{1}H NMR showed peaks that could not be assigned to the desired product or the starting materials.

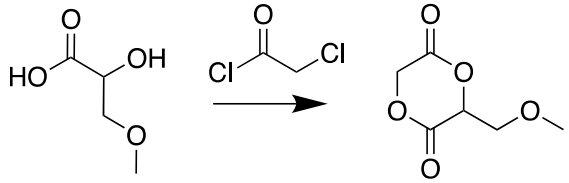

Attempted synthesis of 3-(methoxymethyl)-1,4-dioxane-2,5-dione (**4**): 2-hydroxy-3-methoxypropanoic acid (0.1 g, 0.8 mmol), 2-chloroacetyl chloride (0.06 mL, 0.8 mmol), and freshly distilled triethylamine (2 mL, 14 mmol) were combined in a round-bottomed flask under nitrogen with a stir bar. The mixture was allowed to stir overnight at room temperature. Crude ^{1}H NMR showed peaks that could not be assigned to the desired product or the starting materials.

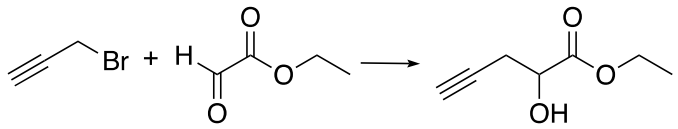

Synthesis of ethyl 2-hydroxypent-4-ynoate (**6**): In an inert atmosphere, 3-bromoprop-1-yne (80% solution in toluene, ~1.5 g) was charged to a dry flask containing Zn (34 g, 0.53 mol) that had been freshly cleaned by 3 M HCl and THF (50 mL). The mixture was stirred at room temperature for 30 minutes, and then cooled in an ice bath. In a separate flask, freshly distilled ethyl 2-oxoacetate (36% solution in toluene via ^{1}H NMR 100 g, 0.352 mol) and 3-bromoprop-1-yne (80% by weight in toluene, 58 g, 0.35 mol) were combined in THF (75 mL) and ether (105 mL). The mixture was added to the slurry dropwise and stirred overnight at 0 °C. The reaction was quenched by addition of HCl (3M, 100 mL) and extracted with ether (3 x 100 mL). The combined organic fractions were dried over $MgSO_4$, filtered and concentrated to produce a brown oil (~100 g) that was purified by column chromatography (30:70 ethyl acetate: hexane). Similar fractions were combined and concentrated via rotary evaporation. Vacuum distillation (70 °C, 24 torr) of the resulting residue produced ethyl 2-hydroxypent-4-ynoate (31.02 g, 55% yield) as a colorless oil. ^{1}H NMR matched that of the reported compound.[4]

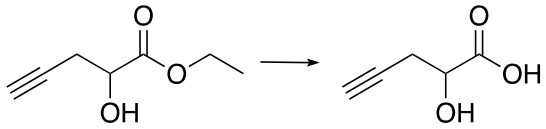

Synthesis of 2-hydroxypent-4-ynoic acid (**7**)*:* Ethyl 2-hydroxypent-4-ynoate (31.02 g, 0.22 mol) and water (350 mL) were charged to a flat-bottom flask. The mixture was refluxed for 3

days. After cooling to room temperature, the reaction was acidified with HCl and continuously extracted for 2 days with ether (300 mL). The brown ether solution was dried over $MgSO_4$, filtered, concentrated by rotary evaporation, and dried overnight under vacuum to give a light brown solid. The brown solid was recrystallized from CH_2Cl_2 in the freezer. The resulting crystals were sublimed (100 mtorr, 60 °C) and recrystallized a second time from CH_2Cl_2 to give white crystals of 2-hydroxypent-4-ynoic acid (9.9 g, 40% yield). ^{1}H NMR matched that of the reported compound.[4]

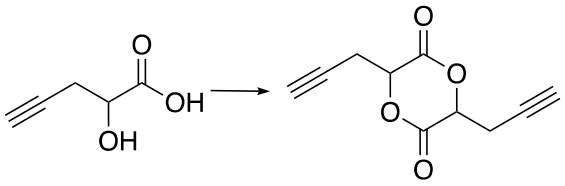

Synthesis of 3,6-di(prop-2-yn-1-yl)-1,4-dioxane-2,5-dione (**8**): 2-Hydroxypent-4-ynoic acid (9.5 g, 83 mmol), toluene, and *p*–toluenesulfonic acid monohydrate (0.82 g, 4 mmol) were charged to a round-bottom flask equipped with a Dean-Stark trap. After 3 days of refluxing, the solvents were removed via rotary evaporation. The brown oil was dissolved in CH_2Cl_2 (300 mL) and washed with saturated $NaHCO_3$ (3 × 50 mL). The organic layer was dried over $MgSO_4$, filtered, and the solvent was removed under vacuum to yield a light brown solid. (~1.81 g). The solid was washed with a small amount of ether and sublimed (300 mtorr, 80 °C). The white crystalline material was then recrystallized from toluene to give pure 3,6-di(prop-2-yn-1-yl)-1,4-dioxane-2,5-dione (1.03 g, 13% yield). ^{1}H NMR matched that of the reported compound.[4]

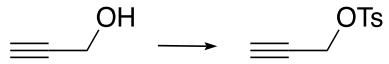

Synthesis of prop-2-yn-1-yl 4-methylbenzenesulfonate: prop-2-yn-1-ol (58 mL, 1 mol) was dissolved dry ether (1L) in a 2 L round bottom flask with a stir bar. Tosyl chloride (250 g 1.3 mol) was added to the stirring mixture under nitrogen. The flask was cooled to 0 °C in a salt water and ice bath. Sodium hydroxide (200 g 5 mol) was added in 6 portions. The round bottom was brought to room temperature overnight. The resulting mixture was poured over ice water and extracted with ether (3 × 250 mL) The ether layer was dried over magnesium sulfate, filtered, and concentrated. Prop-2-yn-1-yl 4-methylbenzenesulfonate was obtained as a dark yellow oil. (191 g, 91 % yield) ^{1}H NMR matched that of the reported compound.[20]

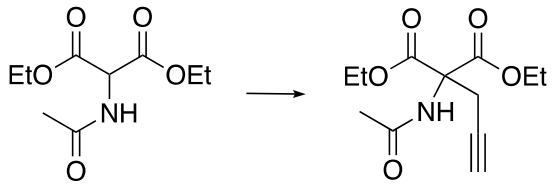

Synthesis of diethyl 2-acetamido-2-(prop-2-yn-1-yl)malonate (**10**): Diethyl 2-acetamidomalonate (105 g, 0.48 mol) was added to a 3 L flame dried 4 necked round-bottomed flask under nitrogen equipped with an overhead stirrer and condenser. Freshly distilled dioxane (1.4 L) was added via syringe. Nitrogen was bubbled through the solution for ~10 minutes while stirring. In a separate dry 1 L round-bottomed flask, potassium *tert*-Butoxide (*t*-buOK, 62 g, 0.55 mol) was dissolved in freshly distilled dioxane (550 mL). After bubbling nitrogen through the solution for a 10 min, it was transferred to the malonate ester dropwise via cannula and allowed to stir for 2 hours at ~40 °C. Nitrogen was bubbled through a separate dry 500 mL round-bottomed flask that was charged with prop-2-yn-1-yl 4-methylbenzenesulfonate (84

mL, 0.5 mol) and freshly distilled dioxane (150 mL) The tosylate was then added to the malonate ester mixture dropwise via cannula. The mixture was brought to refluxed overnight. The following day the reaction was cooled to room temperature, filtered, and concentrated. The brown liquid was then dissolved in 1 L of DCM washed with water (2 × 250 mL), dried over magnesium sulfate, and decolorized with activated carbon. Concentration of the resulting material yielded a light brown solid (87g) in 80% yield. TLC- 50:50 hexane: ethyl acetate (R_f = 0.53) ^{1}H NMR matched that of the reported compound.[20]

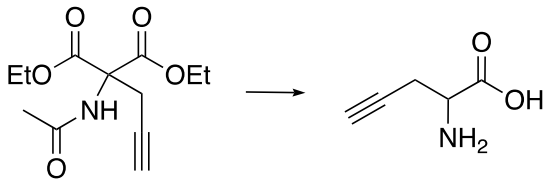

Synthesis of 2-aminopent-4-ynoic acid (**11**): Diethyl 2-acetamidomalonate (34.5 g, 135 mmol) was added to a solution of 2 M H_2SO_4 (375 mL) and brought to reflux. The reaction was monitored by NMR (D_2O 4.15 t 1H, 2.8 m 2H, 1.95 s 1H) for ~36 hours. The mixture was used without further characterization.

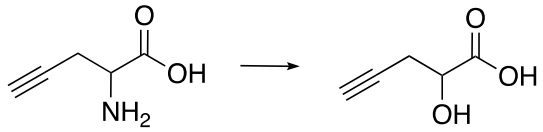

Synthesis of 2-hydroxypent-4-ynoic acid (**7**): A solution of 40% $NaNO_2$ (186 mL) in water was added dropwise to the solution of 2-aminopent-4-ynoic acid at 0 ºC. The mixture was allowed to warm to room temperature overnight and stirred for ~40 hours. Urea in 1 M HCl was added to the mixture until it did not make potassium iodine starch paper turn blue. The mixture was

continuously extracted with ether for 2 days using a 1 L liquid-liquid extractor, concentrated to 250 mL and stirred over $Na_2S_2O_5$ for ~30 minutes the mixture was tested with KI starch paper ever 5 minutes until it did not turn blue/purple (prolonged exposure to atmosphere will eventually discolor the paper) after which it was filtered and concentrated under vacuum to yield a brown solid which was subsequently sublimed under vacuum and recrystallized with DCM to yield colorless crystals (5.41 g, 35% yield) ^{1}H NMR matched that of the reported compound.[20]

Preparation of Si/SiOx wafers: Silicon wafers were cut into 10 x 5 mm small chips washed with a large amount of deionized (DI) water, ethanol, and DI water again. Then the treated silicon substrates were put into an ultraviolet ozone (UVO) cleaner to be oxidized for 30 min to form the silica layer on the silicon.

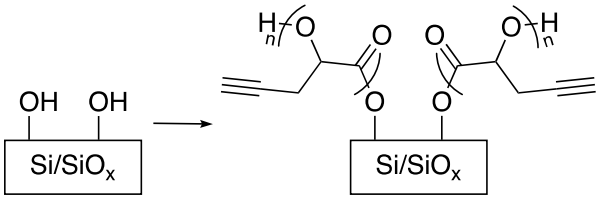

Synthesis of poly(propargylglycolide)polymer brushes: Cut wafers (3 cm × 3 cm) of ingle side polished silicon (wafer world) were washed with water, ethyl acetate, and acetone the wafers were then sonicated in ethanol for 2 minutes dried with a stream of nitrogen then placed into UV-Ozone treatment for 30 minutes. Wafers were immediately moved into the glovebox and added to clean 10 mL vials. In a typical procedure, a solution (0.1 mL of 0.015 M) of tin(II) 2-ethylhexanoate in toluene was added to the wafers followed by a solution of the monomer (1.9

mL of 0.1 M) in toluene. The vials were capped and removed from the glovebox, the caps were wrapped in Teflon tape and electrical tape and the vials were placed on a shaker table at 40 °C for 24 hours. The vials were opened and the wafers were removed and washed with DCM, water, and ethanol. The wafers were sonicated in ethanol and dried with a stream of nitrogen before being used for further experiments and characterization.

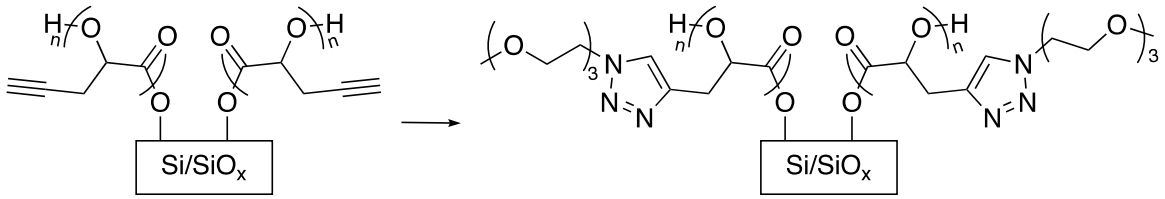

Synthesis of OEG-grafted-poly(propargylglycolide)polymer brushes: Freshly prepared Poly(propargylglycolide) polymer brushes were cleaned with a nitrogen stream and placed into 10 mL vials in a glove box. In a typical procedure, a solution of TEG-azide (0.44 g 2.3 mmol) in 10 mL of DMF was added to a Schlenk flask with sodium ascorbate (0.017 g, 0.094 mmol). The suspension was deoxygenated by 4 freeze-pump-thaw cycles before being transferred into a glove box. A separate solution of $CuSO_4$ (0.078 M) in DMF was also degassed via freeze-pump-thawed and transferred into a glove box. Inside the glove box the OEG-azide and sodium ascorbate suspension (1.8 mL) and the $CuSO_4$ in DMF (0.5 mL) were added to the wafers in the vials. The vials were capped and removed from the glovebox, the caps were wrapped in Teflon tape and electrical tape and the vials were placed on a shaker table at 24 °C for 24 hours. The vials were opened and the wafers were removed and washed with water, and ethanol. The wafers were sonicated in ethanol for 2 min and dried with a stream of nitrogen before being used for further experiments and characterization.

References

(1) Hu, X.; Hu, G.; Crawford, K.; Gorman, C. B. Comparison of the Growth and Degradation of Poly(Glycolic Acid) and Poly(ε-Caprolactone) Brushes. *J. Polym. Sci. Part A Polym. Chem.* **2013**, *51* (21), 4643–4649.

(2) Xu, L.; Gorman, C. B. Poly(Lactic Acid) Brushes Grow Longer at Lower Temperatures. *J. Polym. Sci. Part A Polym. Chem.* **2010**, *48* (15), 3362–3367.

(3) Jiang, X.; Vogel, E. B.; Smith, M. R.; Baker, G. L. Amphiphilic PEG/Alkyl-Grafted Comb Polylactides. *J. Polym. Sci. Part A Polym. Chem.* **2007**, *45* (22), 5227–5236.

(4) Jiang, X.; Vogel, E. B.; Smith, M. R.; Baker, G. L. "Clickable" Polyglycolides: Tunable Synthons for Thermoresponsive, Degradable Polymers. *Macromolecules* **2008**, *41* (6), 1937–1944.

(5) Jiang, X.; Smith, M. R.; Baker, G. L. Water-Soluble Thermoresponsive Polylactides. *Macromolecules* **2008**, *41* (2), 318–324.

(6) Simmons, T. L.; Baker, G. L. Poly(Phenyllactide): Synthesis, Characterization, and Hydrolytic Degradation. *Biomacromolecules* **2001**, *2* (3), 658–663.

(7) Arnold, R. M.; Huddleston, N. E.; Locklin, J. Utilizing Click Chemistry to Design Functional Interfaces through Post-Polymerization Modification. *J. Mater. Chem.* **2012**, *22* (2007), 19357–19365.

(8) Kolb, H. C.; Finn, M. G.; Sharpless, K. B. Click Chemistry: Diverse Chemical Function from a Few Good Reactions. *Angew. Chem. Int. Ed. Engl.* **2001**, *40* (11), 2004–2021.

(9) Lowe, A. B. Thiol–Ene "Click" Reactions and Recent Applications in Polymer and Materials Synthesis: A First Update. *Polym. Chem.* **2014**, *5* (17), 4820.

(10) Lowe, A. B. Thiol-Yne 'Click'/Coupling Chemistry and Recent Applications in Polymer and Materials Synthesis and Modification. *Polymer (Guildf).* **2014**, *55* (22), 5517–5549.

(11) Iha, R. K.; Wooley, K. L.; Nyström, A. M.; Burke, D. J.; Kade, M. J.; Hawker, C. J. Applications of Orthogonal "Click" Chemistries in the Synthesis of Functional Soft Materials. *Chem. Rev.* **2009**, *109* (11), 5620–5686.

(12) Arnold, R. M.; Patton, D. L.; Popik, V. V; Locklin, J. A Dynamic Duo: Pairing Click Chemistry and Postpolymerization Modification to Design Complex Surfaces. *Acc. Chem. Res.* **2014**, *47* (10), 2999–3008.

(13) Zhang, Z.; Yin, L.; Xu, Y.; Tong, R.; Lu, Y.; Ren, J.; Cheng, J. Facile Functionalization of Polyesters through Thiol-Yne Chemistry for the Design of Degradable, Cell-Penetrating and Gene Delivery Dual-Functional Agents. *Biomacromolecules* **2012**, *13* (11), 3456–3462.

(14) Teske, N. S.; Voigt, J.; Shastri, V. P. Clickable Degradable Aliphatic Polyesters via Copolymerization with Alkyne Epoxy Esters: Synthesis and Postfunctionalization with Organic Dyes. *J. Am. Chem. Soc.* **2014**, *136* (29), 10527–10533.

(15) Kalelkar, P. P.; Alas, G. R.; Collard, D. M. Synthesis of an Alkene-Containing Copolylactide and Its Facile Modification by the Addition of Thiols. *Macromolecules* **2016**, *49* (7), 2609–2617.

(16) Pounder, R. J.; Dove, A. P. Towards Poly(Ester) Nanoparticles: Recent Advances in the Synthesis of Functional Poly(Ester)s by Ring-Opening Polymerization. *Polym. Chem.* **2010**, *1* (3), 260–271.

(17) Kimura, Y.; Shirotani, K.; Yamane, H.; Kitao, T. Ring-Opening Polymerization of 3(S)-[(Benzyloxycarbonyl)Methyl]-1,4-Dioxane-2,5-Dione: A New Route to a Poly(α-Hydroxy Acid) with Pendant Carboxyl Groups. *Macromolecules* **1988**, *21* (11), 3338–3340.

(18) Gerhardt, W. W.; Noga, D. E.; Hardcastle, K. I.; García, A. J.; Collard, D. M.; Weck, M. Functional Lactide Monomers: Methodology and Polymerization. *Biomacromolecules* **2006**, *7* (6), 1735–1742.

(19) Trimaille, T.; Möller, M.; Gurny, R. Synthesis and Ring-Opening Polymerization of New Monoalkyl-Substituted Lactides. *J. Polym. Sci. Part A Polym. Chem.* **2004**, *42* (17), 4379–4391.

(20) Zhang, Q.; Ren, H.; Baker, G. L. An Economical and Safe Procedure to Synthesize 2-Hydroxy-4-Pentynoic Acid: A Precursor towards 'Clickable' Biodegradable Polylactide. *Beilstein J. Org. Chem.* **2014**, *10* (1), 1365–1371.

(21) Xu, L.; Crawford, K.; Gorman, C. B. Effects of Temperature and PH on the Degradation of Poly(Lactic Acid) Brushes. *Macromolecules* **2011**, *44* (12), 4777–4782.

(22) Kowalski, A.; Duda, A.; Penczek, S. Kinetics and Mechanism of Cyclic Esters Polymerization Initiated with Tin(II) Octoate. 3. Polymerization of L , L -Dilactide. *Macromolecules* **2000**, *33* (20), 7359–7370.

(23) Kitto, H. J.; Schwartz, E.; Nijemeisland, M.; Koepf, M.; Cornelissen, J. J. L. M.; Rowan, A. E.; Nolte, R. J. M. Post-Modification of Helical Dipeptido Polyisocyanides Using the 'Click' Reaction. *J. Mater. Chem.* **2008**, *18* (46), 5615.

(24) Kim, H.; Kang, Y. J.; Jeong, E. S.; Kang, S.; Kim, K. T. Glucose-Responsive

Disassembly of Polymersomes of Sequence-Specific Boroxole-Containing Block Copolymers under Physiologically Relevant Conditions. *ACS Macro Lett.* **2012**, *1* (10), 1194–1198.

(25) Barbey, R.; Klok, H. A. Room Temperature, Aqueous Post-Polymerization Modification of Glycidyl Methacrylate-Containing Polymer Brushes Prepared via Surface-Initiated Atom Transfer Radical Polymerization. *Langmuir* **2010**, *26* (23), 18219–18230.

(26) Kim, P.; Kim, D. H.; Kim, B.; Choi, S. K.; Lee, S. H.; Khademhosseini, A.; Langer, R.; Suh, K. Y. Fabrication of Nanostructures of Polyethylene Glycol for Applications to Protein Adsorption and Cell Adhesion. *Nanotechnology* **2005**, *16* (10), 2420–2426.

Chapter 4

Introduction

The synthesis and characterization of poly(propargyl glycolide) polymer brushes (PPGL) have been discussed in previous chapters. Here the degradation of PPGL brushes and the oligo(ethylene glycol) side chain derivative (PPGL-OEG) are explored. Additionally, preliminary studies on the protein resistance of the PPGL and the PPGL-OEG are shown. Finally, a time of flight–secondary ion mass spectroscopy (TOF-SIMS) study is presented to explore the efficiency of the click reaction on the polyester backbone as proceeding from the free chain end towards the point of attachment to the substrate.

One of the more interesting and unique characteristics of polyester polymer brushes is that they are degradable under only basic conditions.[1,2] This feature is particularly relevant because physiological pH is generally around 7.4. The controlled degradation of the surfaces could be important for future studies and uses. Initially it was envisioned that this degradation could limit protein adsorption. However, experiments showed that Bovine Serum Albumin (BSA) proteins rapidly adsorbed to the unfunctionalized, polyester surfaces.[3] When block-co-polymers were made utilizing oligo(ethylene glycol) (OEG) the surfaces showed better protein resistance. It was hypothesized that the poly (propargyl glycolide) (PPGL) and poly (propargyl glycolide)-graft-oligo(ethylene glycol) (PPGL-OEG) would have similar degradation profiles as the previously synthesized polyester brushes.

Locklin has reviewed the work of a variety of click reactions on surfaces including polymer brushes but there has not been a detailed study of the efficiency of those reactions on appending groups to polyester brushes.[4] Barbey has shown that the ring opening of epoxides

by small molecule amines is highly efficient via an X-ray photoelectron spectroscopy depth profile study of poly(glycidyl methacrylate) brushes. They further note that proteins such as (BSA) are restricted to the upper layer of the brush and do not intercalate into the brush matrix.[5] Klok and coworkers have studied the effects of modifying poly(2-hydroxyethyl methacrylate) brushes with deuterated amino acids using neutron reflectivity. Their study showed that polar serine was able to distribute homogeneously amongst the brush matrix but nonpolar leucine was immobilized only near the air brush interface.[6]

These results are encouraging because PPGL brushes could be highly functionalized with OEG and have the ability to degrade under physiological conditions as a dual way to resist protein adsorption. The efficiency of post polymerization modification on polyester polymer brushes has had comparably little study.

TOF-SIMS depth profiling presents an opportunity to study the "clicking efficiency" of OEG to the propargyl group on the polymer brushes as a function of height.[7] Click reactions are known to be highly efficient in solution;[8,9] however, the polymer brush matrix presents a sterically congested system that could decrease the efficiency of the reaction or create gradients of functionality.

Results and Discussion

Degradation of PPGL at varying PH

Polypropargyl glycolide brushes were incubated in different pH solutions and removed for thickness measurements. In acidic media (pH = 3.0), the thickness of the brushes increased slightly. In neutral (pH = 7.0) and slight basic (pH = 7.4) media the brush rapidly degraded to 50-60% of its original thickness and maintained that thickness for the duration of the

experiment. In basic media (pH = 8.0) the brush rapidly degraded from the substrate within 25 hours (Figure 16). These results are similar to those observed for poly(ε-caprolactone) (PCL) brushes. In acidic media PCL and PPGL do not degrade. Under highly basic conditions (pH = 8.0) PPGL brushes degrade much faster than PCL (~5 hours for PPGL vs ~50% remaining after 500 hours for PCL). At pH = 7.4 and 7.0 PPGL and PCL brushes have very similar degradations after 500 hours there is about 50% of the brush remaining.[2]

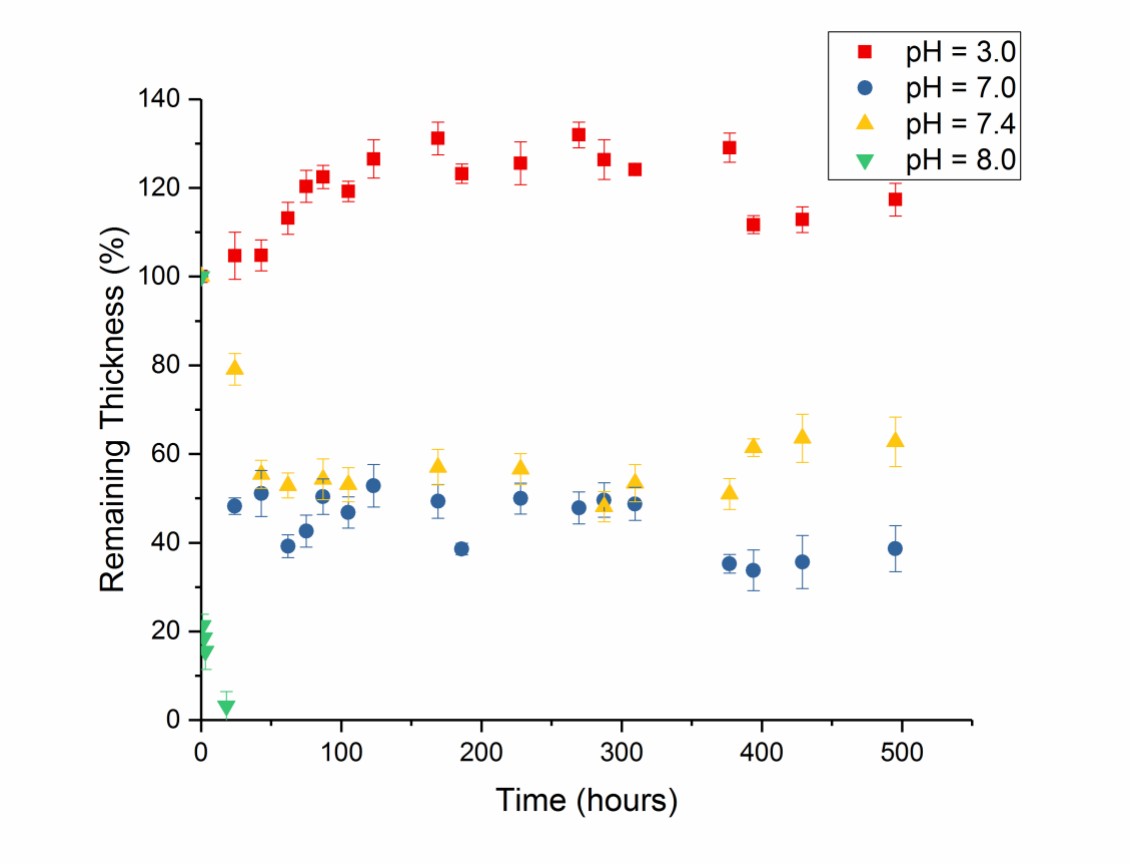

Figure 16: Degradation of PPGL polymer brushes at 25 ˚C in solutions with various pH values.

The increase in thickness observed in acidic conditions could be due to swelling of the polymer brush in the media as it appears to be greater than experimental uncertainty. The initial

rapid degradation observed for slightly basic and neutral media is likely due the degradation of chains near the top of the brush that may not be as densely, packed as the chains at the surface (Figure 17) Additionally, this proposed model could explain the perceived elongation of the chains by ellipsometry if organic impurities were to become trapped in the less dense region near the top of the polymer chains.

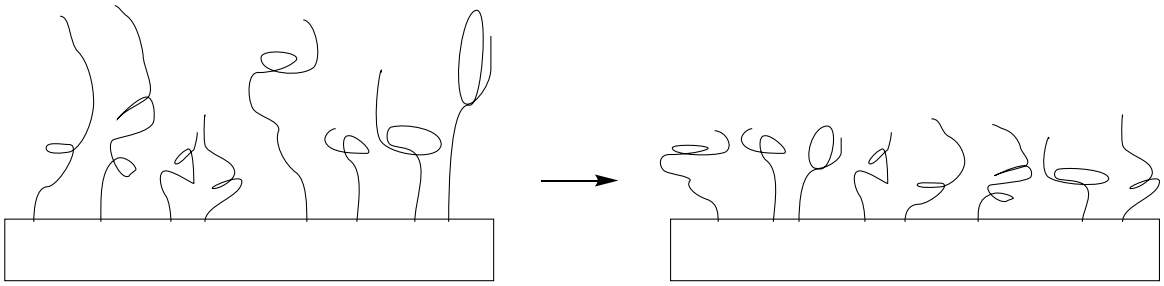

Figure 17: Cartoon depiction of the polydispersity of PPGL polymer brushes while degrading.

Degradation of PPGL-OEG at varying pH

Polypropargyl glycolide (PPGL) brushes that were grafted with diethylene glycol (OEG-PPGL) were incubated in different pH solutions and removed for thickness measurements. In acidic media (pH = 3.0), the thickness of the brushes decreased slightly. In slightly basic (pH = 7.4) media the brush degraded in a nearly linear fashion for ~100 hours before plateauing at around 60% of its original thickness. This 60% thickness was then maintained for the duration of the experiment. In basic media (pH = 8.0) the brush rapidly degraded from the substrate within ~50 hours (Figure 18)

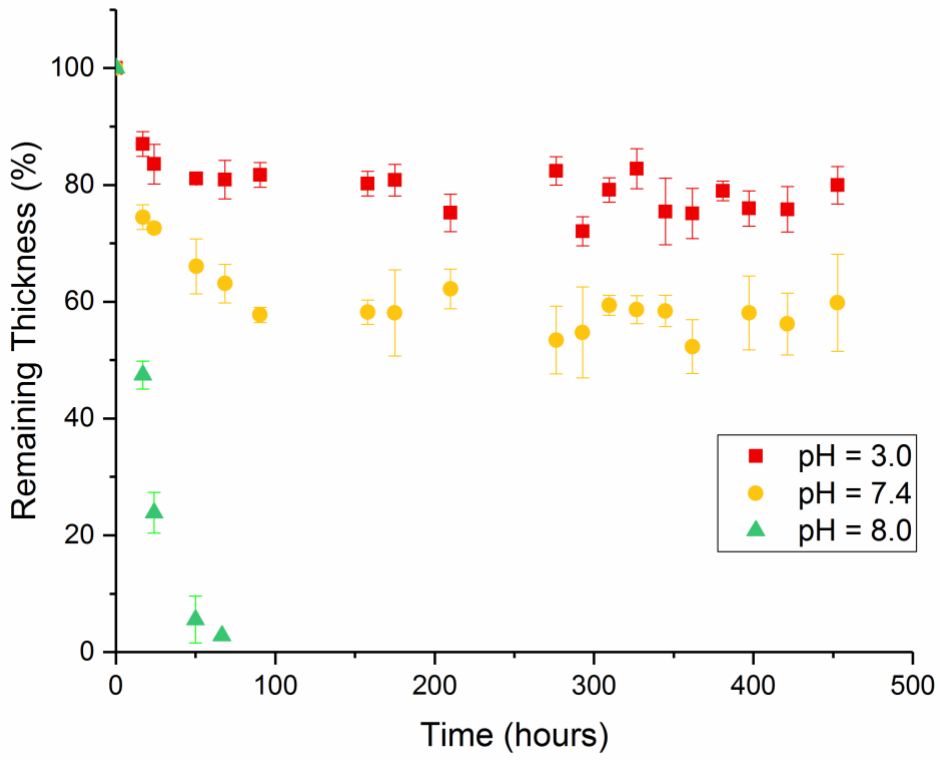

Figure 18: Degradation of OEG-PPGL polymer brush at 25 ˚C in solutions with various pH values.

There are several differences in the degradation of the OEG-PPGL and the PPGL brushes. 1) In acidic media the OEG-PPGL brushes degraded slightly before maintaining a relatively consistent thickness. 2) in highly basic media the length of time to degrade the brush increased by more than a factor of two compared to the PPGL brush. 3) In slightly basic media (pH=7.4) the OEG-PPGL brush displays an almost linear degradation for the first 100 hours but the PPGL brush degraded much more rapidly during that time. In both cases the PPGL and OEG-PPGL thickness did not decrease below 50% of the original thickness during the experiment.

1) This observation could be because of residual impurities remaining on the surface during the initial thickness measurements. Despite rigorous sonication to remove any remaining copper or small DEG-azide some may have remained to artificially increase the perceived thickness of the surface.
2) This observation could also be a result of the steric hindrance caused by the OEG side chain interacting with other polymer brush chains impeding the rate of backbiting.
3) If cartoon representation in Figure 17 is an accurate depiction of the surface, then the upper layer of the brush could degrade rapidly before the active backbiting chains are forced into the denser more sterically hindered lower layer.

These phenomenon differ from what has previously been observed for the degradation of polyester polymer brushes.[2] It is hypothesized that these differences are a result of a higher grafting density in this system. Thus, the individual polymer chains in the brush would take a longer time to degrade -- possibly outside of the time window for these experiments. Additionally, the non-linearity in the decay profiles suggest that there is a fair amount of poly dispersity within these samples.

Preliminary bovine serum albumin (BSA) adsorption studies.

Albumin is the most common serum protein found in whole blood. Bovine serum albumin (BSA) is a commonly used model for albumin in blood. BSA use as a model for protein adsorption is ubiquitous amongst protein resistant surface science literature and it makes a great model system for exploring protein adsorption of surfaces due to its relative ease of handling.[10]

Previously synthesized PPGL and PPGL-OEG polymer brushes were placed in contact with BSA and removed at different periods of time. The wafers were washed with only water so that any adsorbed protein was not removed. Ellipsometric thickness measurements were made of the wafers before they were returned to the buffered BSA solution.

To model the adsorption of BSA on the polymer brushes the degradation profile of PPGL and PPGL-OEG in pH=7.4 phosphate buffer were plotted with the new ellipsometric thickness values associated with the polymer brushes in contact with BSA solution (red lines in Figure 19 and Figure 20). The lower limits (blue lines) represent the initial thickness of the wafer multiplied by the percent of the brush remaining at a time from the degradation profiles (Figure 16 and Figure 18). The thickness of the adsorbed BSA on the surface can then be estimated by the difference between the measured thickness and the estimated degradation in the absence of BSA (grey area). This procedure should give, at best, an overestimate of BSA adsorption as it doesn't account for BSA adsorption slowing the rate of degradation of the underlying brush. The interpretation of these experiments make additional assumptions: 1) the polymer brushes degradation is only influenced by the pH of solution and temperature and 2) incubating BSA with the polymer brush does not lead to a chemical bond between the BSA and the polymer chain. It is suggested that further experiments be carried out to confirm these assumptions (for example incubation of wafers in BSA, followed by removal of BSA via sonication, and examining the ellipsometric thickness of the remaining film compared to the estimated thickness from Figure 18).

PPGL brushes incubated at 25 ˚C showed rapid adsorption of the BSA protein to the surface. (Figure 19) This result is similar to that observed previously on polyester polymer

brushes.[3] Previously, it was hypothesized that the act of degradation may be enough to attenuate the adsorption of BSA. When PPGL brushes are incubated at 37 ˚C they degraded much more rapidly than at 25 ˚C (blue lines in Figure 19). However, despite the initial rapid degradation of the brush, BSA began to accumulate on the surface within 2 hours. This result is consistent with the hydrophobic nature of the PPGL brush. It is also consistent with previously reported data that suggest that degradation alone is not enough to prevent the adsorption of protein[3]

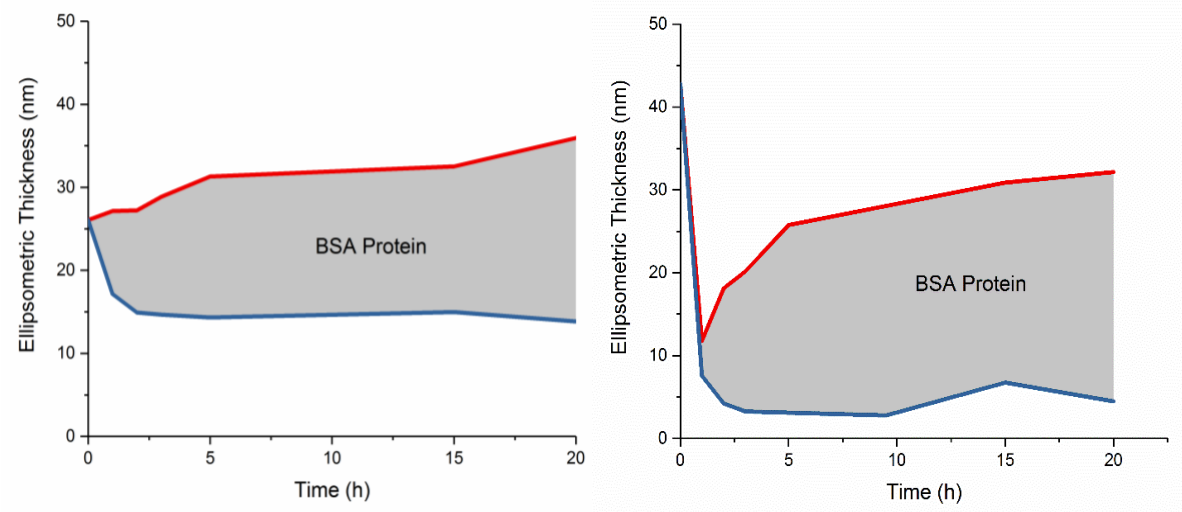

Figure 19: Ellipsometric thickness of PPGL over time at (left 25 ˚C) (right 37 ˚C) pH = 7.4 (blue line), ellipsometric thickness of PPGL brushes incubated with 4.5 mg/mL BSA at pH = 7.4 (red line). Estimated BSA on surface (grey).

The protein resistance of the PPGL-OEG polymer brush was then explored. The OEG side chains that have been grafted to the PPGL brush should help to ward off protein adsorption. In fact, that is what was observed. Significant protein accumulation does not begin until ~18 hours after exposure. Additionally, over the course of the experiment protein accumulation is significantly less than that of the PPGL brushes (grey area of Figure 19). Given

the adsorption of a significant amount of protein starting around 18 hours in the system a study was undertaken to better understand the "clicking efficiency" of the polymer brush. Based on this study PPGL-OEG brushes are able to resist protein adsorption for 18 hours. This result demonstrates a huge improvement over PPGL brushes. When PPGL-OEG brushes are compared to other systems with similar side OEG side chains we see that they perform well when compared to short term studies. We are unaware of literature precedent for longer investigations. The Chilkoti group previously synthesized poly (oligo(ethylene glycol) methacrylate) brushes and showed that they resisted adsorption of flowing fetal bovine serum and a solution of fibronectin for 40 minutes by surface plasmon resonance.[11] Longer incubation times were, however, not reported.

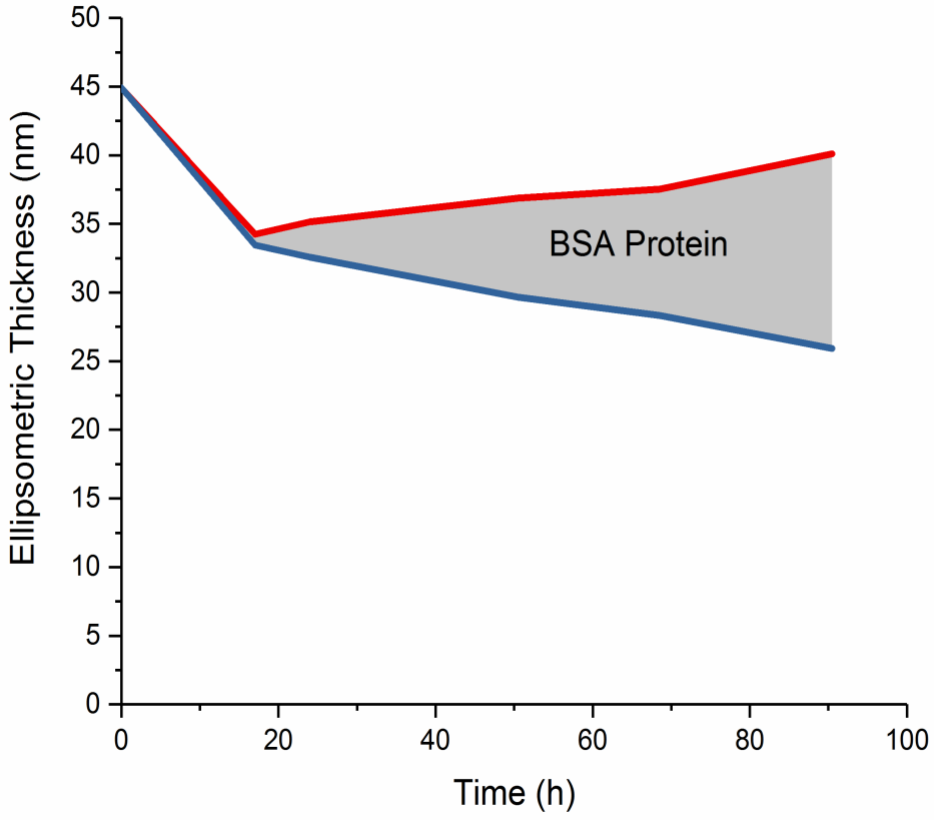

Figure 20: Ellipsometric thickness of PPGL-OEG over time at pH = 7.4 (blue line), ellipsometric thickness of PPGL-OEG brushes incubated with 4.5 mg/mL BSA at pH = 7.4 (red line). Estimated BSA on surface (grey). 25 ˚C

TOF-SIMS to characterize "clicking" efficiency

TOF-SIMS is a surface sensitive technique that can be used to create depth profiles of surfaces. TOF-SIMS has found use in characterizing solar cells,[12] thin films,[13–15] and electronics.[16] The use of C_{60}^{+} as an ion beam is well documented for organic surfaces.[15,17,18] However, there is a relatively small body of literature related to the use of this technique on polymer brushes.[19–21] To the best of our knowledge, the only literature exploring the efficiency

of post-polymerization modification (PPM) reactions on polymer brushes utilized XPS depth profiling[5] and neutron reflectivity.[6]

To better understand the grafting efficiency of OEG to PPGL brushes TOF-SIMS depth profiling was performed on PPGL and PPGL-OEG brushes. Figure 21 shows the negative ion spectra of PPGL brushes over all scans and the positive ion mode spectra of PPGL-OEG. Ion counts were mapped using the ion peak corresponding to $C_5H_3O_2^-$. This peak can be assigned to the monomer unit of the polymer brush. Si^- was used to map the accessibility of the underlying substrate. The ion peak corresponding to CH_3O^+ indicative of the methoxy group of OEG was used to map the "click reaction" efficiency.

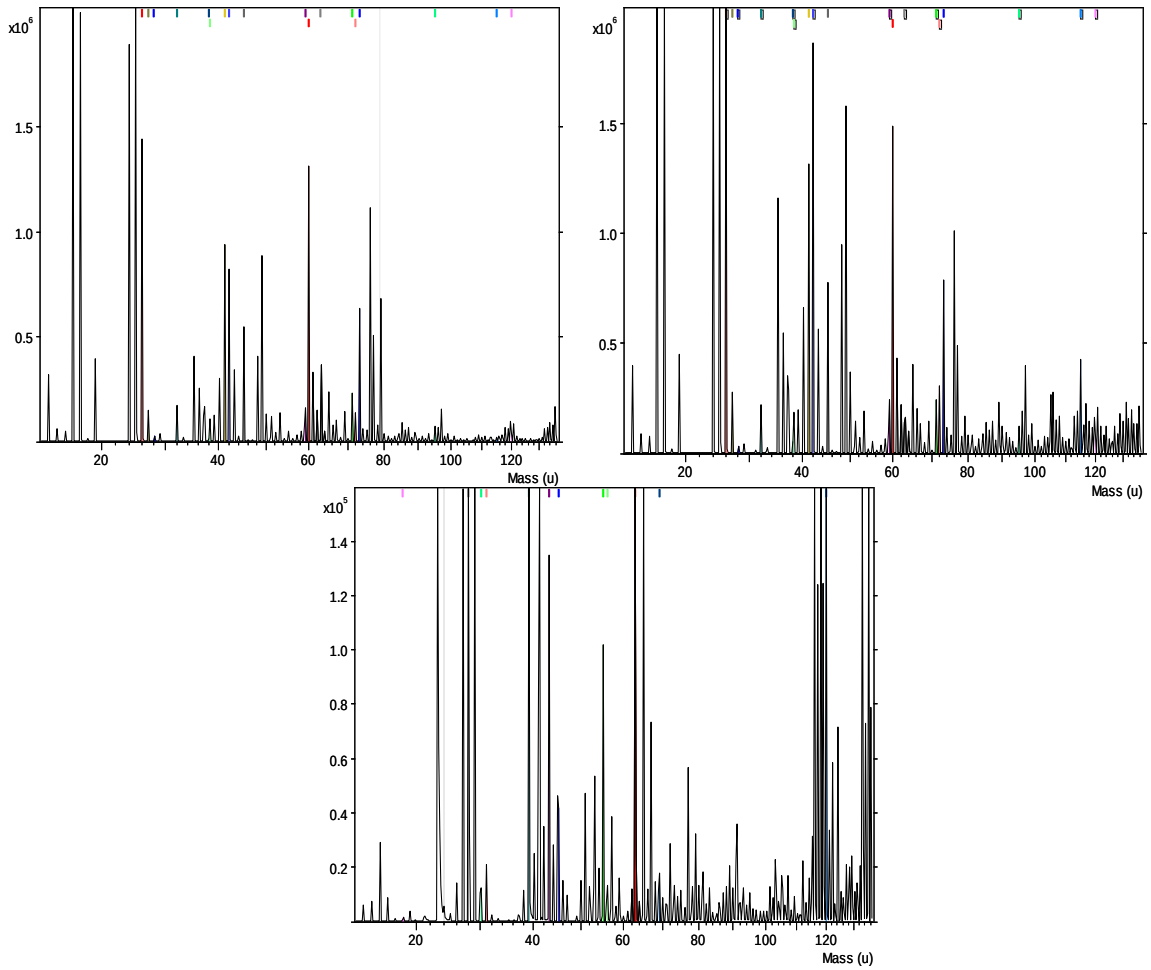

Figure 21: Top left-TOF-SIMS measurement of PPGL negative ion mode. Top right- TOF-SIMS measurement of PPGL-OEG negative ion mode. Bottom- TOF-SIMS measurement of PPGL-OEG positive ion mode

The intensity of $C_5H_3O_2^-$ and Si^- vs sputter time are shown in Figure 23 It takes about 110 seconds to reach the silicon substrate by bombarding it with 10 keV C_{60} ions. This value indicates an approximate sputtering rate for PPGL brushes of 11.6 nm min^{-1}. This value is consistent with the sputtering rate of poly(glycidyl methacrylate) (8.5 nm min^{-1})[5] and poly(methyl methacrylate) (13 nm min^{-1}).[17]

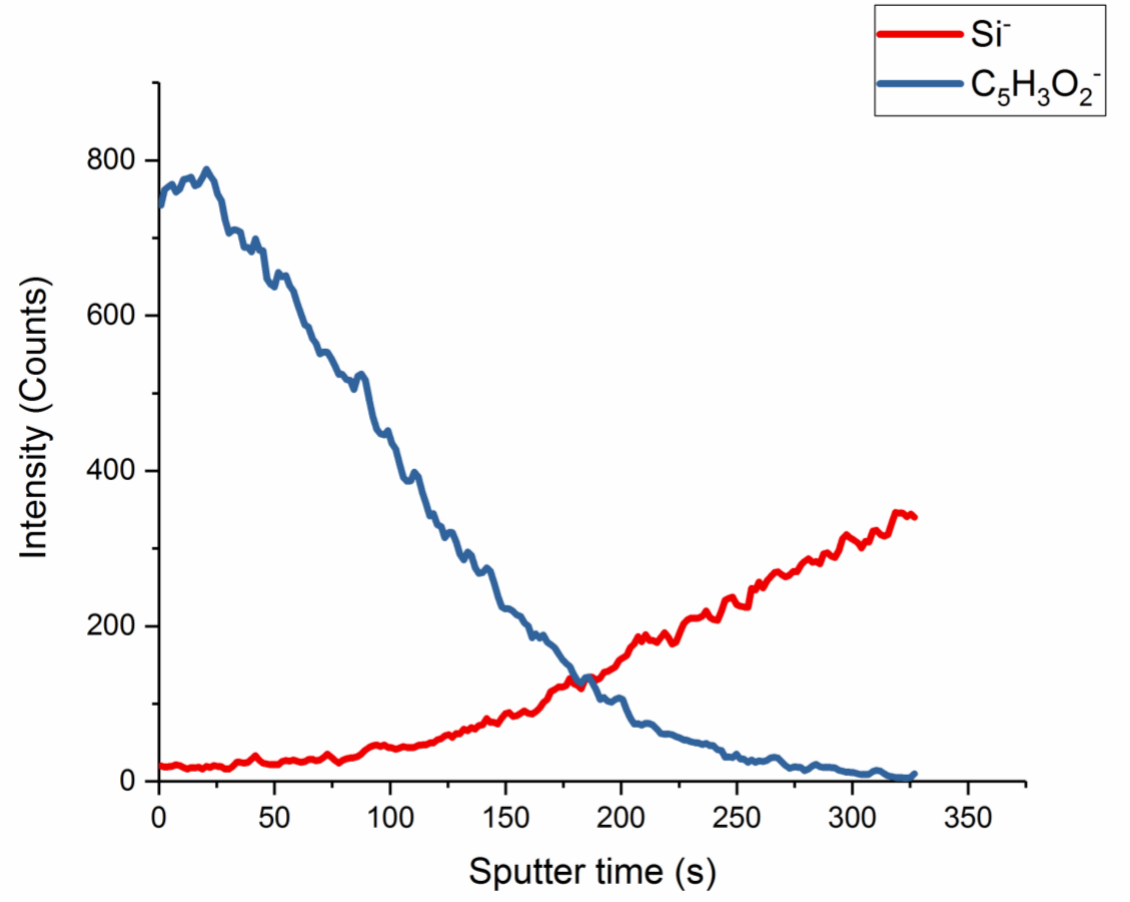

Figure 22: C60 Depth profile of PPGL polymer brush

Figure 23 shows ion map of the monomer unit $C_5H_3O_2^-$ from all scans. The relative uniformity of the surface indicates that the brush has completely covered the silicon wafer. It also shows that there is almost no detection of Si^- in the first 5 nm of the depth profiling, providing further evidence of uniform brush coverage.

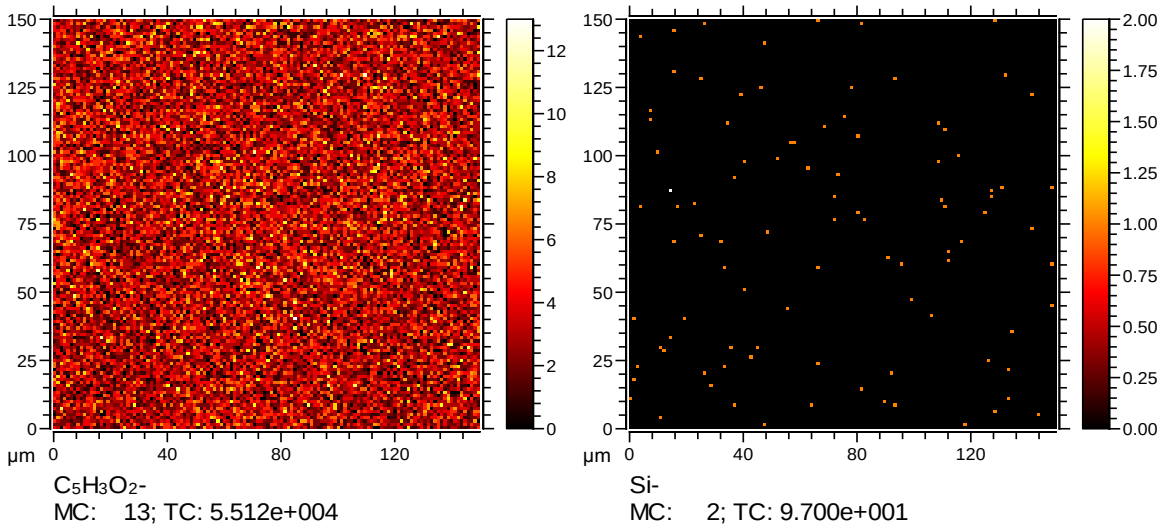

Figure 23: Left ion map of C5H3O2- on PPGL all scans (325 seconds of sputtering). Right ion map of Si- on PPGL first ~5 nm (25 seconds of sputtering) in negative ion mode

Figure 24 shows 3D renderings of the total ion maps for $C_5H_3O_2^-$ and Si^-. The z-axis is sputter time (and thus depth assuming a linear decrease in depth versus time). The concentration of $C_5H_3O_2^-$ decreased as one sputters through the brush and into the surface while the concentration of Si^- increased. This result is consistent with the removal of the brush from the surface and sputtering into the underlying silicon wafer.

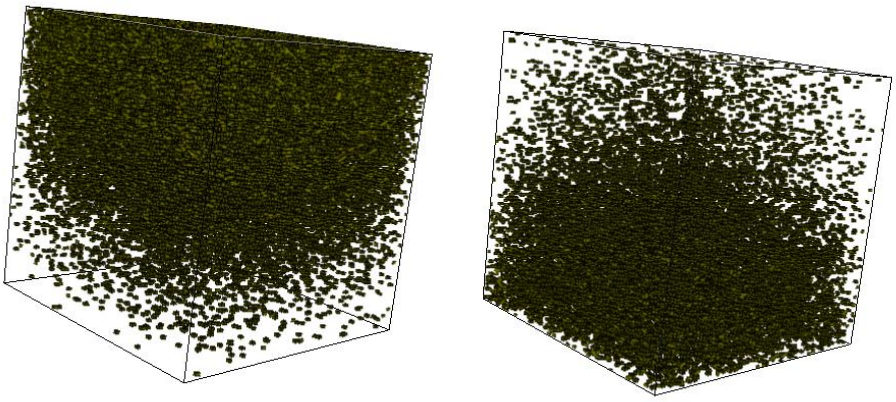

Figure 24: 3D rendering where the z-axis is the depth of removal of the polymer brush and the xy-plane shows ion counts for various positions along the surface at that depth of C5H3O2- (left) and Si- (right) in negative ion mode.

Figure 25 shows the concentration of CH_3O^+ also decreased as the first 25 nm of the brush was removed. The top of the brush is highly functionalized with CH_3O^+ ions while the bottom has less functionalization. This result can be attributed to the need for copper as well as the OEG-azide to diffuse into the brush. While Barbey[5] has shown that small molecule amines have no problem penetrating the polymer brush layer of poly(glycidyl methacrylate) brushes, these results suggest that the OEG-azide or the copper ions may not penetrate the brush layer as well.

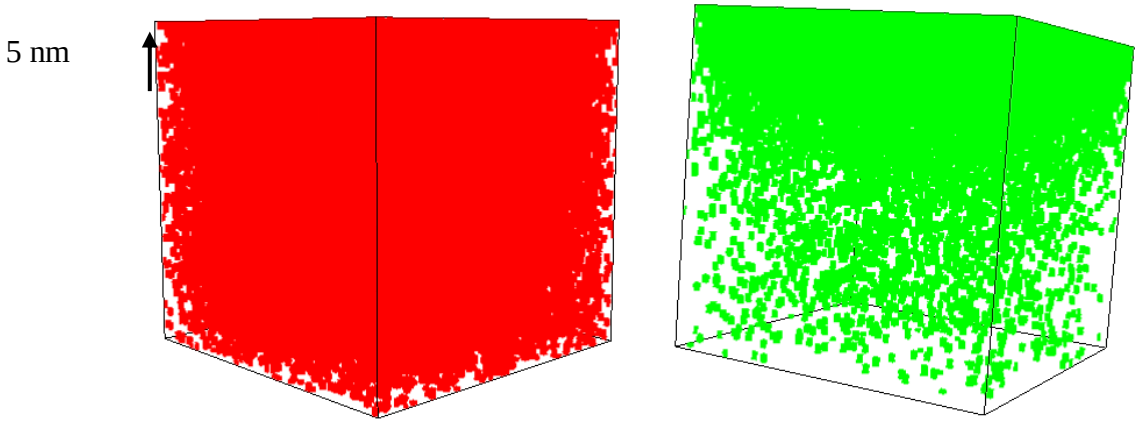

Figure 25: 3D rendering of ion maps of C5H3O2- (left) and CH3O+ (right) through the first 80 scans. The z-axis of each box is 25 nm.

Mapping of the residual Cu^- ion showed that it was found throughout the remaining polymer brush suggesting that copper ions had no problem penetrating the brush layer (Figure 26). Thus, two explanations for the gradient of OEG along the PPGL backbone are suggested. 1) the steric hindrance of neighboring side chains created higher activation barriers for the click reaction due to steric congestion and thus the azide and alkyne were not able to react as efficiently further into the brush layer. 2) the upper portion of the brush is more easily accessible to the cyclization reaction because of the poly disperse nature of the brush (left side of Figure 17).

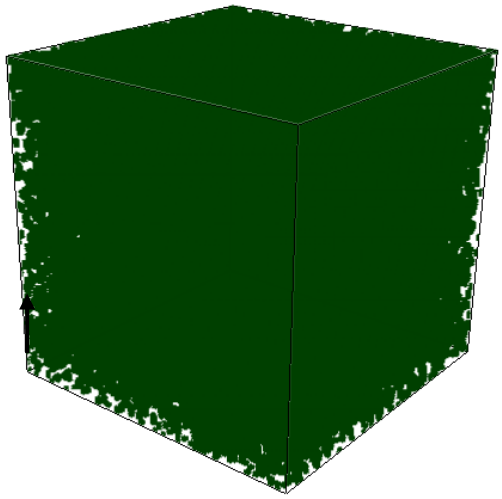

Figure 26: First 80 scans of Cu- ion map. The z-axis of the box is 25 nm. Arrow represents 5 nm on z-axis.

To better understand the depth or gradient of the grafted OEG side chains the integrated (across slabs in the xy-plane) ion peak associated with CH_3O^+ was plotted with the $C_5H_3O_2^-$ peak from PPGL (Figure 27) The ion peak for CH_3O^+ rapidly degraded away while the ion peak associated with $C_5H_3O_2^-$ degraded at a much slower rate. These data imply that the OEG grafts do not penetrate the whole way into the brush as proceeding from the chain ends toward the surface. In fact, most of the grafting occurs in the top 8 nm of the brush. This behavior can be attributed to the looser packing density, increased polydispersity, and the additional chain mobility within the system as one proceeds further away from the silicon substrate.

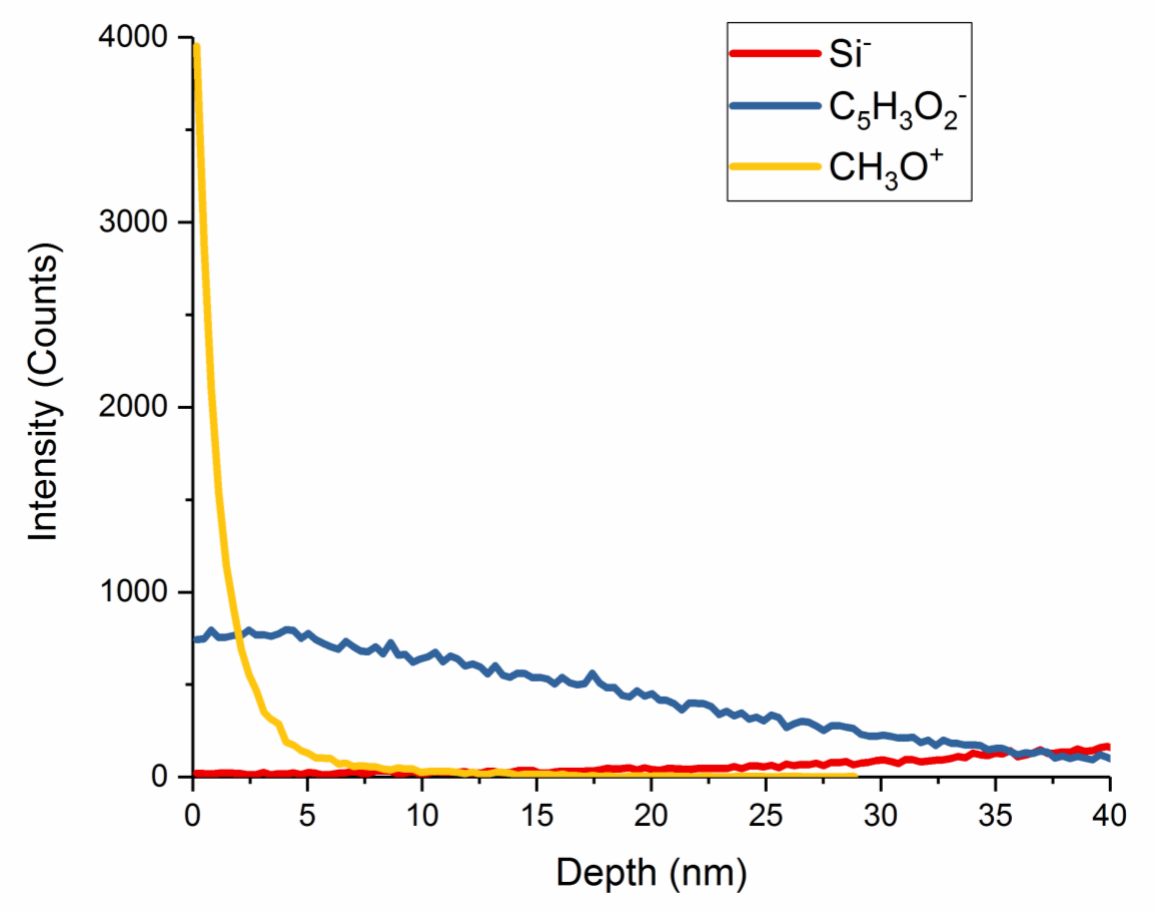

Figure 27: TOF-SIMS depth profile of Si- (red) and C5H3O2- (blue) of PPGL and CH3O+ of PPGL-OEG polymer brushes.

The lower grafting density of OEG in lower regions of the brush may help to explain the protein adsorption that is illustrated in Figure 20. After the first ~12 nm of the PPGL-OEG brush degrade (those containing the highest grafting density of OEG) proteins begin to rapidly adsorb to the surface. These data suggest that the lower regions (those closer to the surface) have a high grafting density preventing OEG from reacting. These data contrast data shown for an XPS depth profile of poly (glycidyl methacrylate) brushes where the authors where able to show full functionalization with propylamine.[5] A few reasons for this dramatic difference

are suggested. 1) The grafting density of PPGL brushes are higher than that of poly (glycidyl methacrylate) brushes– this would result in denser packed chains thus limiting diffusion into the polymer brush matrix. 2. The propylamine is much smaller than OEG and is able to penetrate the brush matrix easier. It is worth noting that when poly (glycidyl methacrylate) brushes were exposed to BSA protein the proteins (assuming functionalization with lysine residues) where restricted to the top 10 nm of the brush. 3. Longer reaction times might allow for higher functionalization of the surface.

In conclusion, the degradation profile of PPGL and PPGL-OEG brushes have been explored. It is suggested that the poly dispersity in the brushes results in the unusual degradation kinetics. This may be attributed to looser packing in the upper regions of the brush allowing for greater water access. Greater water access in polyester thin films has been shown to increase degradation rates.[22]

This proposed looser packing density in the upper region of the brush can be viewed as advantageous in that it allowed for greater grafting density of OEG side chains; however, it also resulted in a faster rate of degradation. Modulating the growth conditions and grafting functionalities in this brush could allow for interesting molecular assemblies of block copolymer brushes where rapid degradation followed by slower degradation are desirable.

Preliminary experiments showed that PPGL brushes will adsorb BSA protein at 25 and 37 ˚C. When OEG is grafted to PPGL a reduction in the amount of BSA adsorbed to the surface is observed; however, at longer exposure times BSA adsorbs to the surface. This may be a result of the gradient of OEG-grafted side chains as proceeding from the free chain end towards the point of attachment to the substrate surface as noted in the TOF-SIMS data.

Experimental

Degradation Studies: Previously synthesized polymer brushes on silicon wafers and 5 mL of phosphate buffered solution were placed into 20 mL scintillation vials. The vials were subsequently capped, placed on a shaker table (rpm = 200), and allowed to stir at given temperature. After a period of time, wafers were removed from the vials, washed with water and ethanol, sonicated for 2 min in ethanol, washed with water and dried under a stream of nitrogen. Each point is the average of 3 ellipsometric thickness measurements on a single wafer. The wafers were then returned to the vials and the process was repeated for additional time points.

Protein Adsorption Studies: Previously synthesized polymer brushes on silicon wafers and 5 mL of 4.5 mg/L bovine serum albumin in pH =7.4 phosphate buffered solution were placed into 20 mL scintillation vials. The vials were subsequently capped, placed on a shaker table (rpm = 200), and allowed to stir at given temperature. After a period of time, wafers were removed from the vials, washed with water and 3 measurements of the ellipsometric thickness on a single wafer were averaged. The wafers were then returned to the vials and, after they incubated for additional time, the process was repeated.

TOF SIMS: Experiment performed in conjunction with the analytical instrumentation facility on North Carolina State University's campus. This experimental procedure is a modification of a standard procedure found at (https://www.aif.ncsu.edu/tof-sims/) ToF-SIMS analyses were conducted using a TOF SIMS V (ION TOF, Inc. Chestnut Ridge, NY) instrument

equipped with a Bi_n^{m+}(n = 1 -5, m = 1, 2) liquid metal ion gun, C_{60}^+ sputtering gun and electron flood gun for charge compensation. Both the Bi and C_{60} ion columns are oriented at 45° with respect to the sample surface normal. The instrument vacuum system consists of a load lock for rapid sample loading and an analysis chamber, separated by the gate valve. The analysis chamber pressure is maintained below 5.0 x 10^{-9} mbar to avoid contamination of the surfaces to be analyzed. For depth profiles acquired in this study, 10 keV C_{60}^+ with 0.4 nA current was used to create an 800 μm by 800 μm area, and the middle 150 μm by 150 μm area was analyzed using 0.3 pA Bi_3^+ primary ion beam. The negative secondary ion mass spectra were calibrated using H^-, C^-, O^-, C_3^-, C_5^- and C_7^-. The positive secondary ion mass spectra were calibrated using H^+, C^+, $C_2H_3^+$, $C_3H_5^+$ and $C_4H_7^+$.

References

(1) Xu, L.; Crawford, K.; Gorman, C. B. Effects of Temperature and PH on the Degradation of Poly(Lactic Acid) Brushes. *Macromolecules* **2011**, *44* (12), 4777–4782.

(2) Hu, X.; Hu, G.; Crawford, K.; Gorman, C. B. Comparison of the Growth and Degradation of Poly(Glycolic Acid) and Poly(ε-Caprolactone) Brushes. *J. Polym. Sci. Part A Polym. Chem.* **2013**, *51* (21), 4643–4649.

(3) Hu, X.; Gorman, C. B. Resisting Protein Adsorption on Biodegradable Polyester Brushes. *Acta Biomater.* **2014**, *10* (8), 3497–3504.

(4) Arnold, R. M.; Huddleston, N. E.; Locklin, J. Utilizing Click Chemistry to Design Functional Interfaces through Post-Polymerization Modification. *J. Mater. Chem.* **2012**, *22* (37), 19357–19365.

(5) Barbey, R.; Laporte, V.; Alnabulsi, S.; Klok, H.-A. A. Postpolymerization Modification of Poly(Glycidyl Methacrylate) Brushes: An XPS Depth-Profiling Study. *Macromolecules* **2013**, *46* (15), 6151–6158.

(6) Schüwer, N.; Geue, T.; Hinestrosa, J. P.; Klok, H. A. Neutron Reflectivity Study on the Postpolymerization Modification of Poly(2-Hydroxyethyl Methacrylate) Brushes. *Macromolecules* **2011**, *44* (17), 6868–6874.

(7) Ren, X.; Weng, L. T.; Fu, Y.; Ng, K. M.; Chan, C. M. Investigating the Chain Conformations of Spin-Coated Polymer Thin Films by ToF-SIMS Depth Profiling. *Surf. Interface Anal.* **2015**, *47* (10), 953–960.

(8) Zhao, P.; Yan, Y.; Feng, X.; Liu, L.; Wang, C.; Chen, Y. Highly Efficient Synthesis of Polymer Brushes with PEO and PCL as Side Chains via Click Chemistry. *Polymer*

(Guildf). **2012**, *53* (10), 1992–2000.

(9) Kalelkar, P. P.; Alas, G. R.; Collard, D. M. Synthesis of an Alkene-Containing Copolylactide and Its Facile Modification by the Addition of Thiols. *Macromolecules* **2016**, *49* (7), 2609–2617.

(10) Norde, W.; Gags, D. Interaction of Bovine Serum Albumin and Human Blood Plasma with PEO-Tethered Surfaces: Influence of PEO Chain Length, Grafting Density, and Temperature. *Langmuir* **2004**, *20* (10), 4162–4167.

(11) Ma, H.; Wells, M.; Beebe, T. P.; Chilkoti, A. Surface-Initiated Atom Transfer Radical Polymerization of Oligo(Ethylene Glycol) Methyl Methacrylate from a Mixed Self-Assembled Monolayer on Gold. *Adv. Funct. Mater.* **2006**, *16* (5), 640–648.

(12) Bulle-Lieuwma, C. W. T.; van Gennip, W. J. H.; van Duren, J. K. J.; Jonkheijm, P.; Janssen, R. A. J.; Niemantsverdriet, J. W. Characterization of Polymer Solar Cells by TOF-SIMS Depth Profiling. *Appl. Surf. Sci.* **2003**, *203–204*, 547–550.

(13) Brison, J.; Muramoto, S.; Castner, D. G. ToF-SIMS Depth Profiling of Organic Films: A Comparison between Single-Beam and Dual-Beam Analysis. *J. Phys. Chem. C* **2010**, *114* (12), 5565–5573.

(14) Cheng, J.; Winograd, N. Depth Profiling of Peptide Films with TOF-SIMS and a C_{60} Probe. *Anal. Chem.* **2005**, *77* (11), 3651–3659.

(15) Wilson, R. G.; Stevie, F. A.; Magee, C. W. *Appendix E of Secondary Ion Mass Spectrometry: A Practical Handbook for Depth Profiling and Bulk Impurity Analysis*; Wiley: New York :, 1989.

(16) Alberici, S. G.; Zonca, R.; Pashmakov, B. Ti Diffusion in Chalcogenides: A ToF-SIMS

Depth Profile Characterization Approach. *Appl. Surf. Sci.* **2004**, *231–232*, 821–825.

(17) Szakal, C.; Sun, S.; Wucher, A.; Winograd, N. C_{60} Molecular Depth Profiling of a Model Polymer. *Appl. Surf. Sci.* **2004**, *231–232*, 183–185.

(18) Hinder, S. J.; Lowe, C.; Watts, J. F. ToF-SIMS Depth Profiling of a Complex Polymeric Coating Employing a C_{60} Sputter Source. *Surf. Interface Anal.* **2007**, *39* (6), 467–475.

(19) Kingshott, P.; Wei, J.; Bagge-Ravn, D.; Gadegaard, N.; Gram, L. Covalent Attachment of Poly(Ethylene Glycol) to Surfaces, Critical for Reducing Bacterial Adhesion. *Langmuir* **2003**, *19* (17), 6912–6921.

(20) Pasche, S.; De Paul, S. M.; Vörös, J.; Spencer, N. D.; Textor, M. Poly(l-Lysine)-Graft-Poly(Ethylene Glycol) Assembled Monolayers on Niobium Oxide Surfaces: A Quantitative Study of the Influence of Polymer Interfacial Architecture on Resistance to Protein Adsorption by ToF-SIMS and in Situ OWLS. *Langmuir* **2003**, *19* (22), 9216–9225.

(21) Navarro, M.; Benetti, E. M.; Zapotoczny, S.; Planell, J. A.; Vancso, G. J. Buried, Covalently Attached RGD Peptide Motifs in Poly(Methacrylic Acid) Brush Layers: The Effect of Brush Structure on Cell Adhesion. *Langmuir* **2008**, *24* (19), 10996–11002.

(22) Lu, L.; Garcia, C. A.; Mikos, A. G. In Vitro Degradation of Thin Poly(DL-Lactic-Co-Glycolic Acid) Films. *J. Biomed. Mater. Res.* **1999**, *46* (2), 236–244.